

MIKE 3 Wave Model FM

Hydrodynamic module

Scientific Documentation



DHI A/S headquarters

Agern Allé 5
DK-2970 Hørsholm
Denmark

+45 4516 9200 Telephone

mike@dhigroup.com

www.mikepoweredbydhi.com

Company Registration No.: DK36466871

PLEASE NOTE

COPYRIGHT

This document refers to proprietary computer software, which is protected by copyright. All rights are reserved. Copying or other reproduction of this manual or the related programmes is prohibited without prior written consent of DHI A/S (hereinafter referred to as "DHI"). For details please refer to your 'DHI Software License Agreement'.

LIMITED LIABILITY

The liability of DHI is limited as specified in your DHI Software License Agreement:

In no event shall DHI or its representatives (agents and suppliers) be liable for any damages whatsoever including, without limitation, special, indirect, incidental or consequential damages or damages for loss of business profits or savings, business interruption, loss of business information or other pecuniary loss arising in connection with the Agreement, e.g. out of Licensee's use of or the inability to use the Software, even if DHI has been advised of the possibility of such damages.

This limitation shall apply to claims of personal injury to the extent permitted by law. Some jurisdictions do not allow the exclusion or limitation of liability for consequential, special, indirect, incidental damages and, accordingly, some portions of these limitations may not apply.

Notwithstanding the above, DHI's total liability (whether in contract, tort, including negligence, or otherwise) under or in connection with the Agreement shall in aggregate during the term not exceed the lesser of EUR 10.000 or the fees paid by Licensee under the Agreement during the 12 months' period previous to the event giving rise to a claim.

Licensee acknowledge that the liability limitations and exclusions set out in the Agreement reflect the allocation of risk negotiated and agreed by the parties and that DHI would not enter into the Agreement without these limitations and exclusions on its liability. These limitations and exclusions will apply notwithstanding any failure of essential purpose of any limited remedy.

CONTENTS

MIKE 3 Wave Model FM Hydrodynamic Module Scientific Documentation

1	Introduction.....	1
2	Governing equations.....	3
2.1	Governing equations in a Cartesian coordinate system	3
2.1.1	Navier-Stokes equations	3
2.1.2	Turbulence model	5
2.2	Governing equations in a sigma coordinate system	10
2.2.1	Navier-Stokes equations	11
2.2.2	Turbulence model	13
3	Numerical method	15
3.1	Mesh and discretization scheme.....	15
3.1.1	Mesh.....	15
3.1.2	Discretization scheme	19
3.2	Finite volume method.....	20
3.3	Numerical solution of the Navier-Stokes equations	20
3.3.1	Space discretization	20
3.3.2	Time integration	23
3.3.3	Poisson equation.....	24
3.3.4	Flooding and drying.....	25
3.3.5	Sponge layer	26
3.3.6	Internal wave generation.....	27
3.3.7	Boundary conditions.....	28
3.4	Numerical solution of the Transport equations	28
3.4.1	Spatial discretization	28
3.4.2	Time integration	29
3.4.3	Boundary conditions.....	29
3.5	Time stepping procedure	29
4	Physics	31
4.1	Eddy viscosity	31
4.2	Bed resistance	31
4.3	Wall friction.....	32
4.4	Vegetation	33
4.5	Porosity	33
5	Parallelization	35
5.1	The domain decomposition	35
5.2	Data exchange	35
5.3	Input and output	36

6	References.....	37
----------	------------------------	-----------

APPENDICES

APPENDIX A – Governing equations in spherical coordinates

1 Introduction

This document presents the scientific background for the MIKE 3 Wave Model FM. The objective is to provide the user with a detailed description of the governing equations, numerical discretization and solution methods.

MIKE 3 Wave Model FM can be applied in the following areas:

- Ports and terminals
 - Wave agitation caused by short and long waves
 - Input to dynamic ship mooring analysis (MIKE 21 MA)
- Coastal areas
 - Non-linear wave transformation
 - Surf and swash zone hydrodynamics
 - Wave breaking and run-up
 - Coastal flooding
 - Tsunamis (transient) modelling
- Coastal structures
 - Wave overtopping
 - Wave transmission (and reflection) through porous structures
 - Input to wave load calculation
- Offshore environments
 - Transformation of steep nonlinear waves
 - 3D wave kinematics for structural load calculations

The model is based on the numerical solution of the three-dimensional incompressible Reynolds-averaged Navier-Stokes equations. Thus, the model consists of continuity and momentum equations, and it is closed by a turbulent closure scheme. The free surface is taken into account using a sigma coordinate transformation approach. The spatial discretization of the governing equations in conserved form is performed using a cell-centered finite volume method. The time integration is performed using a semi-implicit scheme. The vertical convective and diffusion terms are discretized using an implicit scheme to remove the stability limitations associated with the vertical resolution. The remaining terms are discretized using a second-order explicit Runge-Kutta scheme. The projection method is employed for the non-hydrostatic pressure. The interface convective fluxes are calculated using a HLLC approximate Riemann solver. This shock-capturing scheme enables robust and stable simulation of flows involving shocks or discontinuities such as bores and hydraulic jumps. This is essential for modelling of waves in the breaking zone or porous structures. The numerical dissipation accounts for the dissipation in the breaking waves.

2 Governing equations

The governing equations are solved in a sigma coordinate system or a combination of sigma coordinate system and a Cartesian coordinate system. For the hybrid system sigma coordinate is used from the free surface to a specified depth, and z-coordinate is used below. The most important advantage using sigma coordinate is the ability to accurately represent the bathymetry and provide consistent resolution near the bed. However, sigma coordinates can suffer from significant errors in the horizontal pressure gradients, advection and mixing terms in areas with sharp topographic changes (steep slopes). These errors can give rise to unrealistic flows. The use of z-level coordinate allows a simple calculation of the horizontal pressure gradients, advection and mixing terms, but the disadvantages are their inaccuracy in representing the bathymetry and that the stair-step representation of the bathymetry can result in unrealistic flow velocities near the bottom.

The governing equations can also be formulated in a spherical coordinate system. For more details, see Appendix A1.

2.1 Governing equations in a Cartesian coordinate system

2.1.1 Navier-Stokes equations

The non-hydrostatic model is based on the incompressible Navier-Stokes equations subject to the assumptions of Boussinesq and with the free surface described by a height function. In a Cartesian coordinate system the local continuity equation is written as

$$\frac{\partial u}{\partial x} + \frac{\partial v}{\partial y} + \frac{\partial w}{\partial z} = 0 \quad (2.1)$$

and the conservative form of the momentum equation can be written

$$\frac{\partial u}{\partial t} + \frac{\partial u^2}{\partial x} + \frac{\partial vu}{\partial y} + \frac{\partial wu}{\partial z} = fv - \frac{1}{\rho_0} \frac{\partial q}{\partial x} - g \frac{\partial \eta}{\partial x} + F_u - F_{vx} + \frac{\partial}{\partial z} \left(\nu_t^v \frac{\partial u}{\partial z} \right) \quad (2.2)$$

$$\frac{\partial v}{\partial t} + \frac{\partial uv}{\partial x} + \frac{\partial v^2}{\partial y} + \frac{\partial wv}{\partial z} = -fu - \frac{1}{\rho_0} \frac{\partial q}{\partial y} - g \frac{\partial \eta}{\partial y} + F_v - F_{vy} + \frac{\partial}{\partial z} \left(\nu_t^v \frac{\partial v}{\partial z} \right) \quad (2.3)$$

$$\frac{\partial w}{\partial t} + \frac{\partial uw}{\partial x} + \frac{\partial vw}{\partial y} + \frac{\partial w^2}{\partial z} = -\frac{1}{\rho_0} \frac{\partial q}{\partial z} + F_w - F_{vz} + \frac{\partial}{\partial z} \left(\nu_t^v \frac{\partial w}{\partial z} \right) \quad (2.4)$$

Here t is the time; x , y and z are the Cartesian coordinates; η is the surface elevation; u , v and w are the velocity components in the x , y and z direction; q is the non-hydrostatic pressure; $f = 2\Omega \sin\phi$ is the Coriolis parameter (Ω is the angular rate of revolution and ϕ the geographic latitude); ν_t^v is the vertical eddy viscosity; g is the gravitational acceleration; ρ_0 , is the reference density of water; $\mathbf{F}_v = (F_{vx}, F_{vy}, F_{vz})$ is the drag force due to vegetation (see section 4.4). Eqs. (2.2)-(2.4) are obtained by splitting the total pressure, p , into a non-hydrostatic and a hydrostatic component, p_H , where

$$p_H = p_A + \rho_0 g (\eta - z) + g \int_z^\eta (\rho - \rho_0) dz \quad (2.5)$$

The atmospheric pressure, p_A , at the free surface is assumed to be constant over the domain, and the density of water, ρ , is assumed to be constant.

The horizontal diffusion terms are described using a gradient-stress relation, which is simplified to

$$F_u = \frac{\partial}{\partial x} \left(2\nu_t^h \frac{\partial u}{\partial x} \right) + \frac{\partial}{\partial y} \left(\nu_t^h \left(\frac{\partial u}{\partial y} + \frac{\partial v}{\partial x} \right) \right) \quad (2.6)$$

$$F_v = \frac{\partial}{\partial x} \left(\nu_t^h \left(\frac{\partial u}{\partial y} + \frac{\partial v}{\partial x} \right) \right) + \frac{\partial}{\partial y} \left(2\nu_t^h \frac{\partial v}{\partial y} \right) \quad (2.7)$$

$$F_w = \frac{\partial}{\partial x} \left(\nu_t^h \frac{\partial w}{\partial x} \right) + \frac{\partial}{\partial y} \left(\nu_t^h \frac{\partial w}{\partial y} \right) \quad (2.8)$$

where ν_t^h is the horizontal eddy viscosity.

The surface and bottom boundary conditions for u , v and w are

at $z = \eta$

$$\frac{\partial \eta}{\partial t} + u \frac{\partial \eta}{\partial x} + v \frac{\partial \eta}{\partial y} - w = 0, \quad \left(\frac{\partial u}{\partial z}, \frac{\partial v}{\partial z} \right) = (0,0) \quad (2.9)$$

at $z = -d$

$$u \frac{\partial d}{\partial x} + v \frac{\partial d}{\partial y} + w = 0, \quad \left(\frac{\partial u}{\partial z}, \frac{\partial v}{\partial z} \right) = \frac{1}{\rho_0 \nu_t^v} (\tau_{bx}, \tau_{by}) \quad (2.10)$$

Here d is the still water depth, and (τ_{bx}, τ_{by}) are the x - and y -components of the bottom stresses.

The total water depth, $h = \eta + d$, is obtained by vertical integration of the local continuity equation and taking into account the boundary condition at the surface and the bottom

$$\frac{\partial h}{\partial t} + \frac{\partial h \bar{u}}{\partial x} + \frac{\partial h \bar{v}}{\partial y} = 0 \quad (2.11)$$

Where \bar{u} and \bar{v} are the depth-averaged velocities

$$h \bar{u} = \int_{-d}^{\eta} u dz, \quad h \bar{v} = \int_{-d}^{\eta} v dz \quad (2.12)$$

In matrix form the continuity equation and the momentum equations may be written

$$\frac{\partial h}{\partial t} + \nabla \cdot \mathbf{F}^c = 0 \quad (2.13)$$

$$\frac{\partial \mathbf{U}}{\partial t} + \nabla \cdot \mathbf{F}^m = \mathbf{S}_h + \mathbf{S}_q \quad (2.14)$$

Here $\mathbf{F}^c = (F_x^c, F_y^c)^T = (h \bar{u}, h \bar{v})^T$, $\mathbf{U} = (u, v, w)^T$ and $\mathbf{F}^m = \mathbf{F}^{mc} - \mathbf{F}^{md} = (\mathbf{F}_x^m, \mathbf{F}_y^m, \mathbf{F}_z^m)^T$.
The flux components and the source terms can be written

$$\mathbf{F}_x^{mc} = \begin{pmatrix} uu + g\eta \\ uv \\ uw \end{pmatrix} \quad \mathbf{F}_y^{mc} = \begin{pmatrix} uv \\ vv + g\eta \\ vw \end{pmatrix} \quad \mathbf{F}_z^{mc} = \begin{pmatrix} uw \\ vw \end{pmatrix} \quad (2.15)$$

$$\mathbf{F}_x^{md} = \begin{pmatrix} 2v_t^h \frac{\partial u}{\partial x} \\ v_t^h \left(\frac{\partial u}{\partial x} + \frac{\partial v}{\partial y} \right) \\ v_t^h \frac{\partial w}{\partial x} \end{pmatrix} \quad \mathbf{F}_y^{md} = \begin{pmatrix} v_t^h \left(\frac{\partial u}{\partial y} + \frac{\partial v}{\partial x} \right) \\ 2v_t^h \frac{\partial v}{\partial y} \\ v_t^h \frac{\partial w}{\partial y} \end{pmatrix} \quad \mathbf{F}_z^{md} = \begin{pmatrix} v_t^v \frac{\partial u}{\partial z} \\ v_t^v \frac{\partial v}{\partial z} \\ v_t^v \frac{\partial w}{\partial z} \end{pmatrix} \quad (2.16)$$

$$\mathbf{S}_h = \begin{pmatrix} fv - F_{vx} \\ -fu - F_{vy} \\ -F_{vz} \end{pmatrix} \quad \mathbf{S}_q = -\frac{1}{\rho_0} \begin{pmatrix} \frac{\partial q}{\partial x} \\ \frac{\partial q}{\partial y} \\ \frac{\partial q}{\partial w} \end{pmatrix} \quad (2.17)$$

If the hydrostatic pressure assumption is applied, the non-hydrostatic pressure will be zero. With this assumption, a three-dimensional, hydrodynamic model can be significantly simplified because the momentum equation in the vertical direction (Eq. (2.4)) can be neglected.

2.1.2 Turbulence model

The turbulence is modelled using an eddy viscosity concept. The eddy viscosity can be described using empirical formula (see section 4.1) or solving a turbulence closure model. In the MIKE 3 Wave Model FM, there are two turbulence models available, namely the k - ε model and the k - ω model; both are two-equations models.

The k-epsilon model

The k - ε model presented here follows Rodi (1980,1984) and has an additional limiter from Larsen and Fuhrman (2018). The model describes k , the specific turbulent kinetic energy and ε , the dissipation rate of turbulent kinetic energy (turbulent dissipation). The eddy viscosity, ν_t , is defined as

$$\nu_t = c_\mu \frac{k^2}{\tilde{\varepsilon}} \quad (2.18)$$

where c_μ is an empirical constant and $\tilde{\varepsilon}$ is a limited version of ε . Solving a system of equations for k and ε results in the eddy viscosity in eq. (2.18) and this value can be used in the momentum equations for the horizontal and/or vertical eddy viscosity, ν_t^h and ν_t^v .

The turbulent kinetic energy, k , and the turbulent dissipation, ε , are obtained from the following transport equations.

$$\frac{\partial k}{\partial t} + \frac{\partial uk}{\partial x} + \frac{\partial vk}{\partial y} + \frac{\partial wk}{\partial z} = F_k + \frac{\partial}{\partial z} \left(\frac{\nu_{t0}^v}{\sigma_k^v} \frac{\partial k}{\partial z} \right) + P_k - \varepsilon \quad (2.19)$$

$$\frac{\partial \varepsilon}{\partial t} + \frac{\partial u\varepsilon}{\partial x} + \frac{\partial v\varepsilon}{\partial y} + \frac{\partial w\varepsilon}{\partial z} = F_\varepsilon + \frac{\partial}{\partial z} \left(\frac{\nu_{t0}^v}{\sigma_\varepsilon^v} \frac{\partial \varepsilon}{\partial z} \right) + P_\varepsilon - c_{2\varepsilon} \frac{\varepsilon^2}{k} \quad (2.20)$$

Here, P_k and P_ε are production terms and F_k and F_ε are horizontal diffusion terms. The details of the various terms are presented in the following.

The production terms are given as

$$P_k = \nu_t p_0 + c_{fk} P_v \quad (2.21)$$

$$P_\varepsilon = c_{1\varepsilon} c_\mu k p_0 + c_{f\varepsilon} \frac{\tilde{\varepsilon}}{k} P_v \quad (2.22)$$

where, $c_{1\varepsilon}$ is a closure coefficient and

$$p_0 = 2 \sum_{i=1}^3 \sum_{j=1}^3 S_{ij} S_{ij} \quad (2.23)$$

where S_{ij} is the mean strain rate tensor defined as

$$S_{ij} = \frac{1}{2} \left(\frac{\partial u_i}{\partial x_j} + \frac{\partial u_j}{\partial x_i} \right), \text{ for } i, j = 1, 2, 3 \quad (2.24)$$

Here, is used the following notation

$$u_1 = u, \quad u_2 = v, \quad u_3 = w \quad (2.25)$$

$$x_1 = x, \quad x_2 = y, \quad x_3 = z \quad (2.26)$$

P_v is the production term due to vegetation and c_{fk} and $c_{f\varepsilon}$ are two weighting coefficients (see section 4.4).

The vertical diffusion terms are given directly in the transport equations for k and ε . The horizontal diffusion terms have a similar form and are given by

$$F_k = \frac{\partial}{\partial x} \left(\frac{\nu_{t0}^h}{\sigma_k^h} \frac{\partial k}{\partial x} \right) + \frac{\partial}{\partial y} \left(\frac{\nu_{t0}^h}{\sigma_k^h} \frac{\partial k}{\partial y} \right) \quad (2.27)$$

$$F_\varepsilon = \frac{\partial}{\partial x} \left(\frac{\nu_{t0}^h}{\sigma_\varepsilon^h} \frac{\partial \varepsilon}{\partial x} \right) + \frac{\partial}{\partial y} \left(\frac{\nu_{t0}^h}{\sigma_\varepsilon^h} \frac{\partial \varepsilon}{\partial y} \right) \quad (2.28)$$

The coefficients σ_k^h , σ_k^v , σ_ε^h and σ_ε^v are closure coefficients. For the diffusion terms is used an unlimited version of the eddy viscosity

$$\nu_{t0}^h = c_\mu \frac{k^2}{\varepsilon}, \quad \nu_{t0}^v = c_\mu \frac{k^2}{\varepsilon} \quad (2.29)$$

If the momentum equations use an empirical formula for either the horizontal or vertical eddy viscosity, that value is also used in the diffusion terms in the turbulence model. This means, that $\nu_{t0}^h = \nu_t^h$ or $\nu_{t0}^v = \nu_t^v$ is used instead of the corresponding expression in eq. (2.29).

To limit the eddy viscosity in regions with nearly-potential flow and stabilize the model, Larsen and Fuhrman (2018) introduced a limited value of the turbulent dissipation ε ,

$$\tilde{\varepsilon} = \max \left[\varepsilon, \lambda_2 \frac{c_{2\varepsilon} p_0}{c_{1\varepsilon} p_\Omega} \varepsilon \right] \quad (2.30)$$

Here, $\lambda_2 = 0.05$ is a limiter coefficient and

$$p_\Omega = 2 \sum_{i=1}^3 \sum_{j=1}^3 \Omega_{ij} \Omega_{ij} \quad (2.31)$$

where Ω_{ij} is the rotation tensor,

$$\Omega_{ij} = \frac{1}{2} \left(\frac{\partial u_i}{\partial x_j} - \frac{\partial u_j}{\partial x_i} \right), \text{ for } i, j = 1, 2, 3 \quad (2.32)$$

Several carefully calibrated empirical coefficients enter the k - ε turbulence model. In the standard k - ε model (Rodi (1984)), they are

$$c_\mu = 0.09, \quad c_{1\varepsilon} = 1.44, \quad c_{2\varepsilon} = 1.92 \quad (2.33)$$

$$\sigma_k^h = \sigma_k^v = 1.0, \quad \sigma_\varepsilon^h = \sigma_\varepsilon^v = 1.3 \quad (2.34)$$

In matrix form, the transport equations for k and ε may be written

$$\frac{\partial \mathbf{U}}{\partial t} + \nabla \cdot \mathbf{F} = \mathbf{S} \quad (2.35)$$

where $\mathbf{U} = (k, \varepsilon)^T$ and $\mathbf{F} = \mathbf{F}^c - \mathbf{F}^d = (\mathbf{F}_x, \mathbf{F}_y, \mathbf{F}_z)^T$. The flux components and the source terms can be written

$$\mathbf{F}_x^c = \begin{pmatrix} uk \\ u\varepsilon \end{pmatrix}, \quad \mathbf{F}_y^c = \begin{pmatrix} vk \\ v\varepsilon \end{pmatrix}, \quad \mathbf{F}_z^c = \begin{pmatrix} wk \\ w\varepsilon \end{pmatrix} \quad (2.36)$$

$$\mathbf{F}_x^d = \begin{pmatrix} \frac{v_{t0}^h}{\sigma_k^h} \frac{\partial k}{\partial x} \\ \frac{v_{t0}^h}{\sigma_\varepsilon^h} \frac{\partial \varepsilon}{\partial x} \end{pmatrix}, \quad \mathbf{F}_y^d = \begin{pmatrix} \frac{v_{t0}^h}{\sigma_k^h} \frac{\partial k}{\partial y} \\ \frac{v_{t0}^h}{\sigma_\varepsilon^h} \frac{\partial \varepsilon}{\partial y} \end{pmatrix}, \quad \mathbf{F}_z^d = \begin{pmatrix} \frac{v_{t0}^v}{\sigma_k^v} \frac{\partial k}{\partial z} \\ \frac{v_{t0}^v}{\sigma_\varepsilon^v} \frac{\partial \varepsilon}{\partial z} \end{pmatrix} \quad (2.37)$$

$$\mathbf{S} = \begin{pmatrix} P_k - \varepsilon \\ P_\varepsilon - c_{2\varepsilon} \frac{\varepsilon^2}{k} \end{pmatrix} \quad (2.38)$$

The k - ω model

The k - ω model presented here is following Larsen and Fuhrman (2018). It extends the model in Wilcox (2008) with an additional limiter. The model describes the specific turbulent kinetic energy, k , and the specific dissipation rate, ω . The eddy viscosity, ν_t , is defined as

$$\nu_t = \frac{k}{\tilde{\omega}} \quad (2.39)$$

where $\tilde{\omega}$ is a limited version of ω . This value of the eddy viscosity can be used in the momentum equations for the horizontal and/or vertical eddy viscosity, ν_t^h and ν_t^v .

The transport equations for the turbulent kinetic energy, k , and the specific dissipation rate, ω , reads

$$\frac{\partial k}{\partial t} + \frac{\partial uk}{\partial x} + \frac{\partial vk}{\partial y} + \frac{\partial wk}{\partial z} = F_k + \frac{\partial}{\partial z} \left(\frac{v_{t0}^v}{\sigma_k^v} \frac{\partial k}{\partial z} \right) + P_k - \beta_k \omega k \quad (2.40)$$

$$\frac{\partial \omega}{\partial t} + \frac{\partial u\omega}{\partial x} + \frac{\partial v\omega}{\partial y} + \frac{\partial w\omega}{\partial z} = F_\omega + \frac{\partial}{\partial z} \left(\frac{v_{t0}^v}{\sigma_\omega^v} \frac{\partial \omega}{\partial z} \right) + F_{\omega c} + P_\omega - \beta_\omega \omega^2 \quad (2.41)$$

Here, F_k and F_ω are horizontal diffusion terms, $F_{\omega c}$ is a cross-diffusion term and P_k and P_ω are production terms. The details of the various terms are presented in the following.

The production terms are given by

$$P_k = v_t p_0 + c_{fk} P_v \quad (2.42)$$

$$P_\omega = \alpha \frac{\omega}{\hat{\omega}} \left(p_0 + \frac{c_{f\omega}}{v_t} P_v \right) \quad (2.43)$$

where $\hat{\omega}$ is a limited version of the specific dissipation rate, ω , α is a closure coefficient and p_0 was defined in eq. (2.23). P_v is the production term due to vegetation and c_{fk} and $c_{f\omega}$ are two weighting coefficients (see section 4.4).

The vertical diffusion terms are given directly in the transport equations for k and ω . The horizontal diffusion terms have a similar form and are given by

$$F_k = \frac{\partial}{\partial x} \left(\frac{v_{t0}^h}{\sigma_k^h} \frac{\partial k}{\partial x} \right) + \frac{\partial}{\partial y} \left(\frac{v_{t0}^h}{\sigma_k^h} \frac{\partial k}{\partial y} \right) \quad (2.44)$$

$$F_\omega = \frac{\partial}{\partial x} \left(\frac{v_{t0}^h}{\sigma_\omega^h} \frac{\partial \omega}{\partial x} \right) + \frac{\partial}{\partial y} \left(\frac{v_{t0}^h}{\sigma_\omega^h} \frac{\partial \omega}{\partial y} \right) \quad (2.45)$$

The coefficients σ_k^h , σ_k^v , σ_ω^h and σ_ω^v are closure coefficients. For the diffusion terms is used an unlimited version of the eddy viscosity

$$v_{t0}^h = \frac{k}{\omega}, \quad v_{t0}^v = \frac{k}{\omega} \quad (2.46)$$

If the momentum equations use an empirical formula for either the horizontal or vertical eddy viscosity, that value is also used in the diffusion terms in the turbulence model. This means, that $v_{t0}^h = v_t^h$ or $v_{t0}^v = v_t^v$ is used instead of the corresponding expression in eq. (2.46). The cross-diffusion term in the equation for ω reads

$$F_{\omega c} = \frac{\sigma_{do}}{\omega} \max \left\{ 0, \frac{\partial k}{\partial x} \frac{\partial \omega}{\partial x} + \frac{\partial k}{\partial y} \frac{\partial \omega}{\partial y} + \frac{\partial k}{\partial z} \frac{\partial \omega}{\partial z} \right\} \quad (2.47)$$

To limit the eddy viscosity in regions with nearly-potential flow and stabilize the model, Larsen and Fuhrman (2018) introduced an additional limiter for ω on top of the limiter already present in the k - ω model from Wilcox (2008). The limited versions of ω are defined as

$$\hat{\omega} = \max \left[\omega, \lambda_1 \sqrt{\frac{p_0 - p_b}{\beta_k}} \right] \quad (2.48)$$

$$\tilde{\omega} = \max \left[\hat{\omega}, \lambda_2 \frac{\beta_\omega p_0}{\beta_k \alpha p_\Omega} \omega \right] \quad (2.49)$$

The values of the limiter coefficients are $\lambda_1 = 0.875$ and $\lambda_2 = 0.05$ and p_Ω was defined in eq. (2.31).

The system contains several empirically determined closure coefficients which have the following values,

$$\sigma_k^h = \sigma_k^v = \frac{5}{3}, \quad \sigma_\omega^h = \sigma_\omega^v = 2, \quad \sigma_{d\omega} = \frac{1}{8} \quad (2.50)$$

$$\alpha = 0.52 \quad (2.51)$$

$$\beta_k = 0.09, \quad \beta_\omega = \beta_0 f_\beta, \quad \beta_0 = 0.0708 \quad (2.52)$$

$$f_\beta = \frac{1 + 85\chi_\omega}{1 + 100\chi_\omega}, \quad \chi_\omega = \left| \frac{\sum_{i=1}^3 \sum_{j=1}^3 \sum_{k=1}^3 \Omega_{ij} \Omega_{jk} S_{ki}}{(\beta_k \omega)^3} \right| \quad (2.53)$$

These values are from Larsen and Fuhrmann (2018), except f_β which is from Wilcox (2008). Larsen and Fuhrman (2018) use $f_\beta = 1$, consistent with two-dimensional flow. Note that β_k corresponds to c_μ in the k - ε model. The mean strain rate tensor S_{ij} and the rotation tensor Ω_{ij} were defined in eq. (2.24) and (2.32).

In matrix form, the transport equations for k and ω may be written as

$$\frac{\partial \mathbf{U}}{\partial t} + \nabla \cdot \mathbf{F} - \mathbf{G} = \mathbf{S} \quad (2.54)$$

where $\mathbf{U} = (k, \omega)^T$ and $\mathbf{F} = \mathbf{F}^c - \mathbf{F}^d = (\mathbf{F}_x, \mathbf{F}_y, \mathbf{F}_z)^T$. The flux components \mathbf{F} , the cross-diffusion \mathbf{G} and the source terms \mathbf{S} can be written

$$\mathbf{F}_x^c = \begin{pmatrix} uk \\ u\omega \end{pmatrix}, \quad \mathbf{F}_y^c = \begin{pmatrix} vk \\ v\omega \end{pmatrix}, \quad \mathbf{F}_z^c = \begin{pmatrix} wk \\ w\omega \end{pmatrix} \quad (2.55)$$

$$\mathbf{F}_x^d = \begin{pmatrix} \frac{v_{t0}^h}{\sigma_k^h} \frac{\partial k}{\partial x} \\ \frac{v_{t0}^h}{\sigma_\omega^h} \frac{\partial \omega}{\partial x} \end{pmatrix}, \quad \mathbf{F}_y^d = \begin{pmatrix} \frac{v_{t0}^h}{\sigma_k^h} \frac{\partial k}{\partial y} \\ \frac{v_{t0}^h}{\sigma_\omega^h} \frac{\partial \omega}{\partial y} \end{pmatrix}, \quad \mathbf{F}_z^d = \begin{pmatrix} \frac{v_{t0}^v}{\sigma_k^v} \frac{\partial k}{\partial z} \\ \frac{v_{t0}^v}{\sigma_\omega^v} \frac{\partial \omega}{\partial z} \end{pmatrix} \quad (2.56)$$

$$\mathbf{G} = \begin{pmatrix} 0 \\ \frac{\sigma_d}{\omega} \max \left[0, \frac{\partial k}{\partial x} \frac{\partial \omega}{\partial x} + \frac{\partial k}{\partial y} \frac{\partial \omega}{\partial y} + \frac{\partial k}{\partial z} \frac{\partial \omega}{\partial z} \right] \end{pmatrix} \quad (2.57)$$

$$\mathbf{S} = \begin{pmatrix} P_k - \beta_k \omega k \\ P_\omega - \beta_\omega \omega^2 \end{pmatrix} \quad (2.58)$$

Boundary conditions at the surface and the seabed

At boundaries where there is a friction, the boundary conditions for k , ε and ω can be modelled with wall functions, Wilcox (1998),

$$k = \frac{1}{\sqrt{\beta_k}} U_\tau^2, \quad \varepsilon = \frac{U_\tau^3}{\kappa \Delta y}, \quad \omega = \frac{U_\tau}{\sqrt{\beta_k} \kappa \Delta y} \quad (2.59)$$

Here, U_τ is the friction velocity associated with the boundary and Δy is the distance from the boundary to the point where the conditions are employed. Furthermore, $\kappa = 0.41$ is the von Kármán constant.

At the seabed, $z = -d$, if there is a bed resistance, the boundary conditions are the wall functions in eq. (2.59) where $\Delta y = \Delta z_b$ is the distance to the bottom and $U_\tau = U_{\tau b}$ is the friction velocity associated with the bottom stress, see section 4.2.

At the surface, $z = \eta$, it is assumed there is no friction, and the boundary conditions are

at $z = \eta$

$$\frac{\partial k}{\partial z} = 0, \quad \varepsilon = \frac{(k\sqrt{c_\mu})^{3/2}}{\alpha_s \kappa h}, \quad \omega = \frac{\sqrt{k}}{\alpha_s \beta_k^{1/4} \kappa h} \quad (2.60)$$

where $\alpha_s = 0.07$ is an empirical constant.

2.2 Governing equations in a sigma coordinate system

The equations are solved using a vertical σ -transformation

$$t' = t, \quad x' = x, \quad y' = y, \quad \sigma = \frac{z + d}{h} \quad (2.61)$$

where σ varies between 0 at the bottom and 1 at the surface. The chain rule is applied to obtain partial derivatives of the function $f = f(t, x, y, z)$

$$\frac{\partial f}{\partial t} = \frac{\partial f}{\partial t'} + \frac{\partial f}{\partial \sigma} \frac{\partial \sigma}{\partial t} \quad (2.62)$$

$$\frac{\partial f}{\partial x} = \frac{\partial f}{\partial x'} + \frac{\partial f}{\partial \sigma} \frac{\partial \sigma}{\partial x} \quad (2.63)$$

$$\frac{\partial f}{\partial y} = \frac{\partial f}{\partial y'} + \frac{\partial f}{\partial \sigma} \frac{\partial \sigma}{\partial y} \quad (2.64)$$

$$\frac{\partial f}{\partial z} = \frac{\partial f}{\partial \sigma} \frac{\partial \sigma}{\partial z} \quad (2.65)$$

where the partial derivatives of σ are given by

$$A_t = \frac{\partial \sigma}{\partial t} = -\frac{1}{h} \Psi_t, \quad \Psi_t = \sigma \frac{\partial h}{\partial t} \quad (2.66)$$

$$A_x = \frac{\partial \sigma}{\partial x} = -\frac{1}{h} \Psi_x, \quad \Psi_x = \sigma \frac{\partial h}{\partial x} - \frac{\partial d}{\partial x} \quad (2.67)$$

$$A_y = \frac{\partial \sigma}{\partial y} = -\frac{1}{h} \Psi_y, \quad \Psi_y = \sigma \frac{\partial h}{\partial y} - \frac{\partial d}{\partial y} \quad (2.68)$$

$$A_z = \frac{\partial \sigma}{\partial z} = \frac{1}{h} \quad (2.69)$$

2.2.1 Navier-Stokes equations

In the sigma coordinate system, the governing equations are given as

$$\frac{\partial h}{\partial t'} + \frac{\partial hu}{\partial x'} + \frac{\partial hv}{\partial y'} + \frac{\partial h\omega}{\partial \sigma} = 0 \quad (2.70)$$

$$\frac{\partial hu}{\partial t'} + \frac{\partial hu^2}{\partial x'} + \frac{\partial hvu}{\partial y'} + \frac{\partial h\omega u}{\partial \sigma} = \quad (2.71)$$

$$fhv - \frac{h}{\rho_0} \left(\frac{\partial q}{\partial x'} + \frac{\partial q}{\partial \sigma} \frac{\partial \sigma}{\partial x} \right) - gh \frac{\partial \eta}{\partial x'} + hF_u - hF_{vx} + \frac{\partial}{\partial \sigma} \left(\frac{v_t^v}{h} \frac{\partial u}{\partial \sigma} \right)$$

$$\frac{\partial hv}{\partial t'} + \frac{\partial huv}{\partial x'} + \frac{\partial hv^2}{\partial y'} + \frac{\partial h\omega v}{\partial \sigma} = \quad (2.72)$$

$$-fhu - \frac{h}{\rho_0} \left(\frac{\partial q}{\partial y'} + \frac{\partial q}{\partial \sigma} \frac{\partial \sigma}{\partial y} \right) - gh \frac{\partial \eta}{\partial y'} + hF_v - hF_{vy} + \frac{\partial}{\partial \sigma} \left(\frac{v_t^v}{h} \frac{\partial v}{\partial \sigma} \right)$$

$$\frac{\partial h\omega}{\partial t'} + \frac{\partial hu\omega}{\partial x'} + \frac{\partial hv\omega}{\partial y'} + \frac{\partial h\omega\omega}{\partial \sigma} = -\frac{1}{\rho_0} \frac{\partial q}{\partial \sigma} + hF_w - hF_{vz} + \frac{\partial}{\partial \sigma} \left(\frac{v_t^v}{h} \frac{\partial \omega}{\partial \sigma} \right) \quad (2.73)$$

The modified vertical velocity, ω , in the sigma coordinate system is given by

$$\omega = \frac{1}{h} \left(w + u \frac{\partial d}{\partial x} + v \frac{\partial d}{\partial y} - \sigma \left(\frac{\partial h}{\partial t} + u \frac{\partial h}{\partial x} + v \frac{\partial h}{\partial y} \right) \right) \quad (2.74)$$

The modified vertical velocity is the velocity across a level of constant σ . The horizontal diffusion terms are approximated by

$$hF_u \approx \frac{\partial}{\partial x} \left(2hv_t^h \frac{\partial u}{\partial x} \right) + \frac{\partial}{\partial y} \left(hv_t^h \left(\frac{\partial u}{\partial y} + \frac{\partial v}{\partial x} \right) \right) \quad (2.75)$$

$$hF_v \approx \frac{\partial}{\partial x} \left(hv_t^h \left(\frac{\partial u}{\partial y} + \frac{\partial v}{\partial x} \right) \right) + \frac{\partial}{\partial y} \left(2hv_t^h \frac{\partial v}{\partial y} \right) \quad (2.76)$$

$$hF_w \approx \frac{\partial}{\partial x} \left(hv_t^h \frac{\partial \omega}{\partial x} \right) + \frac{\partial}{\partial y} \left(hv_t^h \frac{\partial \omega}{\partial y} \right) \quad (2.77)$$

The surface and bottom boundary conditions for u , v and ω are

at $z = \eta$

$$\omega = 0, \quad \left(\frac{\partial u}{\partial \sigma}, \frac{\partial v}{\partial \sigma} \right) = (0,0) \quad (2.78)$$

at $z = -d$

$$\omega = 0, \quad \left(\frac{\partial u}{\partial \sigma}, \frac{\partial v}{\partial \sigma} \right) = \frac{h}{\rho_0 v_t^v} (\tau_{bx}, \tau_{by}) \quad (2.79)$$

The depth-averaged continuity equation becomes

$$\frac{\partial h}{\partial t'} + \frac{\partial h\bar{u}}{\partial x'} + \frac{\partial h\bar{v}}{\partial y'} = 0 \quad (2.80)$$

where \bar{u} and \bar{v} are the depth-averaged velocities

$$\bar{u} = \int_0^1 u d\sigma, \quad \bar{v} = \int_0^1 v d\sigma = 0 \quad (2.81)$$

In matrix form the continuity equations and the momentum equations may be written

$$\frac{\partial h}{\partial t'} + \nabla \cdot \mathbf{F}^c = 0 \quad (2.82)$$

$$\frac{\partial \mathbf{U}}{\partial t'} + \nabla \cdot \mathbf{F}^m = \mathbf{S}_h + \mathbf{S}_q \quad (2.83)$$

where $\mathbf{F}^c = (F_x^c, F_y^c)^T = (h\bar{u}, h\bar{v})^T$, $\mathbf{U} = (hu, hv, hw)^T$ and $\mathbf{F}^m = \mathbf{F}^{mc} - \mathbf{F}^{md} = (\mathbf{F}_x^m, \mathbf{F}_y^m, \mathbf{F}_\sigma^m)^T$.

The flux components and the source terms can be written

$$\mathbf{F}_x^{mc} = \begin{pmatrix} hu u + \frac{1}{2} g(\eta^2 + 2\eta d) \\ huv \\ huw \end{pmatrix} \quad \mathbf{F}_y^{mc} = \begin{pmatrix} huv \\ hvv + \frac{1}{2} g(\eta^2 + 2\eta d) \\ hvw \end{pmatrix} \quad \mathbf{F}_\sigma^{mc} = \begin{pmatrix} hu\omega \\ hv\omega \\ hw\omega \end{pmatrix} \quad (2.84)$$

$$\mathbf{F}_x^{md} = \begin{pmatrix} 2hv_t^h \frac{\partial u}{\partial x} \\ hv_t^h \left(\frac{\partial u}{\partial y} + \frac{\partial v}{\partial x} \right) \\ hv_t^h \frac{\partial w}{\partial x} \end{pmatrix} \quad \mathbf{F}_y^{md} = \begin{pmatrix} hv_t^h \left(\frac{\partial u}{\partial y} + \frac{\partial v}{\partial x} \right) \\ 2hv_t^h \frac{\partial v}{\partial y} \\ hv_t^h \frac{\partial w}{\partial y} \end{pmatrix} \quad \mathbf{F}_\sigma^{md} = \begin{pmatrix} v_t^v \frac{\partial u}{\partial \sigma} \\ h \frac{\partial \sigma}{\partial \sigma} \\ v_t^v \frac{\partial v}{\partial \sigma} \\ h \frac{\partial \sigma}{\partial \sigma} \\ v_t^v \frac{\partial w}{\partial \sigma} \\ h \frac{\partial \sigma}{\partial \sigma} \end{pmatrix} \quad (2.85)$$

$$\mathbf{S}_h = \begin{pmatrix} g\eta \frac{\partial d}{\partial x'} + fhv - hF_{vx} \\ g\eta \frac{\partial d}{\partial y'} - fhu - hF_{vy} \\ -hF_{vz} \end{pmatrix} \quad \mathbf{S}_q = -\frac{1}{\rho_0} \begin{pmatrix} h \left(\frac{\partial q}{\partial x'} + \frac{\partial q}{\partial \sigma} \frac{\partial \sigma}{\partial x} \right) \\ h \left(\frac{\partial q}{\partial y'} + \frac{\partial q}{\partial \sigma} \frac{\partial \sigma}{\partial y} \right) \\ \frac{\partial q}{\partial \sigma} \end{pmatrix} \quad (2.86)$$

To give a conservative formulation, the gravity surface terms are split into two terms (see Chippada (1998), Rogers (2001), Quecedo (2002), Liang or Borthwick (2009))

$$gh \frac{\partial \eta}{\partial x'} = \frac{1}{2} g \frac{\partial (h^2 - d^2)}{\partial x'} - g\eta \frac{\partial d}{\partial x'} = \frac{1}{2} g \frac{\partial (\eta^2 + 2\eta d)}{\partial x'} - g\eta \frac{\partial d}{\partial x'} \quad (2.87)$$

$$gh \frac{\partial \eta}{\partial y'} = \frac{1}{2}g \frac{\partial(h^2 - d^2)}{\partial y'} - g\eta \frac{\partial d}{\partial y'} = \frac{1}{2}g \frac{\partial(\eta^2 + 2\eta d)}{\partial y'} - g\eta \frac{\partial d}{\partial y'} \quad (2.88)$$

It is easily seen that if η is constant, the two terms cancel exactly. In the discrete case, this is also true if the two derivatives are calculated using the same scheme.

2.2.2 Turbulence model

The k-epsilon model

In the sigma coordinate system, the transport equations for the k - ϵ model are given as

$$\frac{\partial hk}{\partial t'} + \frac{\partial huk}{\partial x'} + \frac{\partial hvk}{\partial y'} + \frac{\partial h\omega k}{\partial \sigma} = hF_k + \frac{\partial}{\partial \sigma} \left(D_k^v \frac{\partial k}{\partial z} \right) + h(P_k - \epsilon) \quad (2.89)$$

$$\frac{\partial h\epsilon}{\partial t'} + \frac{\partial hu\epsilon}{\partial x'} + \frac{\partial hv\epsilon}{\partial y'} + \frac{\partial h\omega\epsilon}{\partial \sigma} = hF_\epsilon + \frac{\partial}{\partial \sigma} \left(D_\epsilon^v \frac{\partial \epsilon}{\partial z} \right) + h \left(P_\epsilon - c_{2\epsilon} \frac{\epsilon^2}{k} \right) \quad (2.90)$$

where $D_k^v = \nu_{t0}^v / \sigma_k^v$ and $D_\epsilon^v = \nu_{t0}^v / \sigma_\epsilon^v$ are the vertical diffusion coefficients. Denoting the horizontal diffusion coefficients with $D_k^h = \nu_{t0}^h / \sigma_k^h$ and $D_\epsilon^h = \nu_{t0}^h / \sigma_\epsilon^h$, the horizontal diffusion terms are defined as

$$hF_k = \frac{\partial}{\partial x'} \left(hD_k^h \frac{\partial k}{\partial x} \right) - \frac{\partial}{\partial \sigma} \left(\Psi_x D_k^h \frac{\partial k}{\partial x} \right) + \frac{\partial}{\partial y'} \left(hD_k^h \frac{\partial k}{\partial y} \right) - \frac{\partial}{\partial \sigma} \left(\Psi_y D_k^h \frac{\partial k}{\partial y} \right) \quad (2.91)$$

$$hF_\epsilon = \frac{\partial}{\partial x'} \left(hD_\epsilon^h \frac{\partial \epsilon}{\partial x} \right) - \frac{\partial}{\partial \sigma} \left(\Psi_x D_\epsilon^h \frac{\partial \epsilon}{\partial x} \right) + \frac{\partial}{\partial y'} \left(hD_\epsilon^h \frac{\partial \epsilon}{\partial y} \right) - \frac{\partial}{\partial \sigma} \left(\Psi_y D_\epsilon^h \frac{\partial \epsilon}{\partial y} \right) \quad (2.92)$$

In matrix form, the transport equations for k and ϵ may be written

$$\frac{\partial \mathbf{U}}{\partial t'} + \nabla \cdot \mathbf{F} = \mathbf{S} \quad (2.93)$$

where $\mathbf{U} = (hk, h\epsilon)^T$ and $\mathbf{F} = \mathbf{F}^c - \mathbf{F}^d = (\mathbf{F}_x, \mathbf{F}_y, \mathbf{F}_\sigma)^T$. The flux components and the source terms can be written

$$\mathbf{F}_x^c = \begin{pmatrix} huk \\ hu\epsilon \end{pmatrix}, \quad \mathbf{F}_y^c = \begin{pmatrix} hvk \\ hv\epsilon \end{pmatrix}, \quad \mathbf{F}_\sigma^c = \begin{pmatrix} h\omega k \\ h\omega\epsilon \end{pmatrix} \quad (2.94)$$

$$\mathbf{F}_x^d = \begin{pmatrix} hD_k^h \frac{\partial k}{\partial x} \\ hD_\epsilon^h \frac{\partial \epsilon}{\partial x} \end{pmatrix}, \quad \mathbf{F}_y^d = \begin{pmatrix} hD_k^h \frac{\partial k}{\partial y} \\ hD_\epsilon^h \frac{\partial \epsilon}{\partial y} \end{pmatrix}, \quad \mathbf{F}_\sigma^d = \begin{pmatrix} D_k^v \frac{\partial k}{\partial z} - \Psi_x D_k^h \frac{\partial k}{\partial x} - \Psi_y D_k^h \frac{\partial k}{\partial y} \\ D_\epsilon^v \frac{\partial \epsilon}{\partial z} - \Psi_x D_\epsilon^h \frac{\partial \epsilon}{\partial x} - \Psi_y D_\epsilon^h \frac{\partial \epsilon}{\partial y} \end{pmatrix} \quad (2.95)$$

$$\mathbf{S} = \begin{pmatrix} h(P_k - \epsilon) \\ h \left(P_\epsilon - c_{2\epsilon} \frac{\epsilon^2}{k} \right) \end{pmatrix} \quad (2.96)$$

The k-omega model

In this section, the modified vertical velocity in the sigma coordinate system is called w_s (instead of ω). This is to distinguish it from the specific dissipation rate, ω , of turbulent

kinetic energy which was introduced in section 2.1.2. In the sigma coordinate system, the transport equations for the k - ω model are given as

$$\frac{\partial hk}{\partial t'} + \frac{\partial huk}{\partial x'} + \frac{\partial hvk}{\partial y'} + \frac{\partial hw_s k}{\partial \sigma} = hF_k + \frac{\partial}{\partial \sigma} \left(D_k^v \frac{\partial k}{\partial z} \right) + h(P_k - \beta_k \omega k) \quad (2.97)$$

$$\frac{\partial h\omega}{\partial t'} + \frac{\partial hu\omega}{\partial x'} + \frac{\partial hv\omega}{\partial y'} + \frac{\partial hw_s \omega}{\partial \sigma} = hF_\omega + \frac{\partial}{\partial \sigma} \left(D_\omega^v \frac{\partial \omega}{\partial z} \right) + hF_{\omega c} + h(P_\omega - \beta_\omega \omega^2) \quad (2.98)$$

where $D_k^v = \nu_{t0}^v / \sigma_k^v$ and $D_\omega^v = \nu_{t0}^v / \sigma_\omega^v$ are the vertical diffusion coefficients. Denoting the horizontal diffusion coefficients with $D_k^h = \nu_{t0}^h / \sigma_k^h$ and $D_\omega^h = \nu_{t0}^h / \sigma_\omega^h$, the horizontal diffusion terms are defined as

$$hF_k = \frac{\partial}{\partial x'} \left(hD_k^h \frac{\partial k}{\partial x} \right) - \frac{\partial}{\partial \sigma} \left(\Psi_x D_k^h \frac{\partial k}{\partial x} \right) + \frac{\partial}{\partial y'} \left(hD_k^h \frac{\partial k}{\partial y} \right) - \frac{\partial}{\partial \sigma} \left(\Psi_y D_k^h \frac{\partial k}{\partial y} \right) \quad (2.99)$$

$$hF_\omega = \frac{\partial}{\partial x'} \left(hD_\omega^h \frac{\partial \omega}{\partial x} \right) - \frac{\partial}{\partial \sigma} \left(\Psi_x D_\omega^h \frac{\partial \omega}{\partial x} \right) + \frac{\partial}{\partial y'} \left(hD_\omega^h \frac{\partial \omega}{\partial y} \right) - \frac{\partial}{\partial \sigma} \left(\Psi_y D_\omega^h \frac{\partial \omega}{\partial y} \right) \quad (2.100)$$

In matrix form, the transport equations for k and ω may be written

$$\frac{\partial \mathbf{U}}{\partial t'} + \nabla \cdot \mathbf{F} - \mathbf{G} = \mathbf{S} \quad (2.101)$$

where $\mathbf{U} = (hk, h\omega)^T$ and $\mathbf{F} = \mathbf{F}^c - \mathbf{F}^d = (\mathbf{F}_x, \mathbf{F}_y, \mathbf{F}_\sigma)^T$. The flux components \mathbf{F} , the cross-diffusion \mathbf{G} and the source terms \mathbf{S} can be written

$$\mathbf{F}_x^c = \begin{pmatrix} huk \\ hu\omega \end{pmatrix}, \quad \mathbf{F}_y^c = \begin{pmatrix} hvk \\ hv\omega \end{pmatrix}, \quad \mathbf{F}_\sigma^c = \begin{pmatrix} hw_s k \\ hw_s \omega \end{pmatrix} \quad (2.102)$$

$$\mathbf{F}_x^d = \begin{pmatrix} hD_k^h \frac{\partial k}{\partial x} \\ hD_\omega^h \frac{\partial \omega}{\partial x} \end{pmatrix}, \quad \mathbf{F}_y^d = \begin{pmatrix} hD_k^h \frac{\partial k}{\partial y} \\ hD_\omega^h \frac{\partial \omega}{\partial y} \end{pmatrix}, \quad \mathbf{F}_\sigma^d = \begin{pmatrix} D_k^v \frac{\partial k}{\partial z} - \Psi_x D_k^h \frac{\partial k}{\partial x} - \Psi_y D_k^h \frac{\partial k}{\partial y} \\ D_\omega^v \frac{\partial \omega}{\partial z} - \Psi_x D_\omega^h \frac{\partial \omega}{\partial x} - \Psi_y D_\omega^h \frac{\partial \omega}{\partial y} \end{pmatrix} \quad (2.103)$$

$$\mathbf{G} = \begin{pmatrix} 0 \\ hF_{\omega c} \end{pmatrix} \quad (2.104)$$

$$\mathbf{S} = \begin{pmatrix} h(P_k - \varepsilon) \\ h(P_\omega - \beta_\omega \omega^2) \end{pmatrix} \quad (2.105)$$

3 Numerical method

The discretization in solution domain is performed using a cell-centered finite volume method (CCFV). The spatial domain is discretized by subdivision of the continuum into non-overlapping control volumes and by evaluating the field equations in integral form on these cells.

3.1 Mesh and discretization scheme

3.1.1 Mesh

The computational mesh is based on the unstructured meshes approach, which gives the maximum degree of flexibility. Control of node distribution allows for optimal usage of nodes and adaptation of mesh resolution to the relevant physical scales. The use of unstructured meshes also makes it possible to handle problems characterized by computational domains with complex boundaries.

The 3D mesh is a layered mesh. In the horizontal domain an unstructured mesh is used while in the vertical domain a structured mesh is used (see Figure 3.1). The elements are prisms with either a 3-sided or 4-sided polygonal base. Hence, the horizontal faces are either triangles or quadrilateral elements. The elements are perfectly vertical, and all layers have identical horizontal topology.

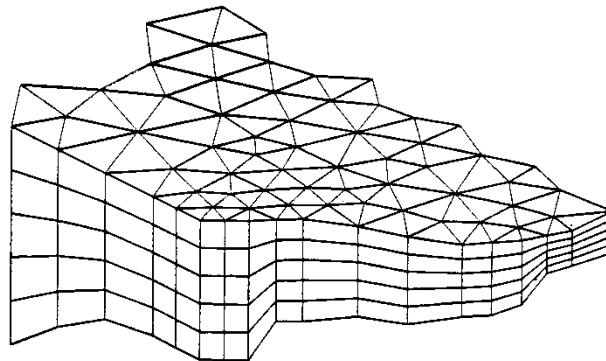


Figure 3.1 Principle of meshing

For the vertical discretization both a standard sigma discretization and a combined sigma/z-level discretization can be used. For the hybrid sigma/z-level discretization, sigma coordinates are used from the free surface to a specified depth, z_0 , and z-level coordinates are used below. The different types of vertical discretization are illustrated in Figure 3.2. At least one sigma layer is needed using the sigma/z-level discretization to allow changes in the surface elevation.

Sigma

In the sigma domain a constant number of layers, N_σ , is used, and the height of each sigma layer is a fixed fraction of the total depth of the sigma domain, h_σ , where $h_\sigma = \eta - \max(z_b, z_\sigma)$. The discretization in the sigma domain is given by a number of discrete σ -levels $\{\sigma_i, i = 1, (N_\sigma + 1)\}$. Here σ varies from $\sigma_1 = 0$ at the bottom interface of the lowest sigma layer to $\sigma_{N_\sigma+1} = 1$ at the free surface.

Variable sigma coordinates can be obtained using a discrete formulation of the general vertical coordinate (s-coordinate) system proposed by Song and Haidvogel (1994). First an equidistant discretization in an s-coordinate system ($-1 \leq s \leq 0$) is defined

$$s_i = -\frac{N_\sigma + 1 - i}{N_\sigma} \quad i = 1, (N_\sigma + 1) \quad (3.1)$$

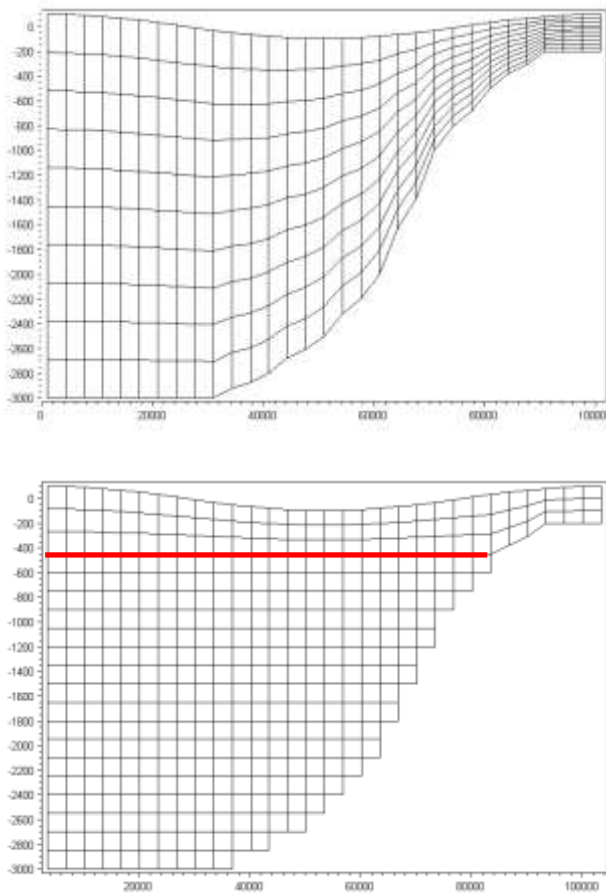


Figure 3.2 Illustrations of the different vertical grids. Upper: sigma mesh, Lower: combined sigma/z-level mesh with simple bathymetry adjustment. The red line shows the interface between the z-level domain and the sigma-level domain

The discrete sigma coordinates can then be determined by

$$\sigma_i = 1 + \sigma_c s_i + (1 - \sigma_c) c(s_i) \quad i = 1, (N_\sigma + 1) \quad (3.2)$$

where

$$c(s) = (1 - b) \frac{\sinh(\theta s)}{\sinh(\theta)} + b \frac{\tanh\left(\theta\left(s + \frac{1}{2}\right)\right) - \tanh\left(\frac{\theta}{2}\right)}{2 \tanh\left(\frac{\theta}{2}\right)} \quad (3.3)$$

Here σ_c is a weighting factor between the equidistant distribution and the stretch distribution, θ is the surface control parameter, and b is the bottom control parameter. The

range for the weighting factor is $0 < \sigma_c \leq 1$ where the value 1 corresponds to equidistant distribution, and 0 corresponds to stretched distribution. A small value of σ_c can result in linear instability. The range of the surface control parameter is $0 < \theta < 20$, and the range of the bottom control parameter is $0 \leq b \leq 1$. If $\theta \ll 1$ and $b = 0$, an equidistant vertical resolution is obtained. By increasing the value of θ , the highest resolution is achieved near the surface. If $\theta > 0$ and $b = 1$, a high resolution is obtained both near the surface and near the bottom.

Examples of a mesh using variable vertical discretization are shown in Figure 3.3 and Figure 3.4.

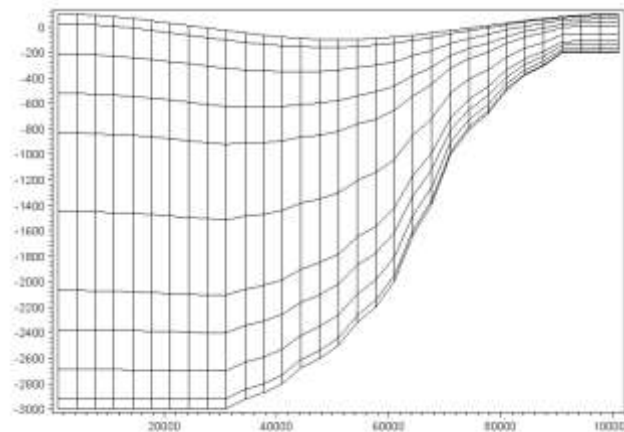


Figure 3.3 Example of vertical distribution using layer thickness distribution. Number of layers: 10, thickness of layers 1 to 10: .025, 0.075, 0.1, 0.01, 0.02, 0.02, 0.1, 0.1, 0.075, 0.025

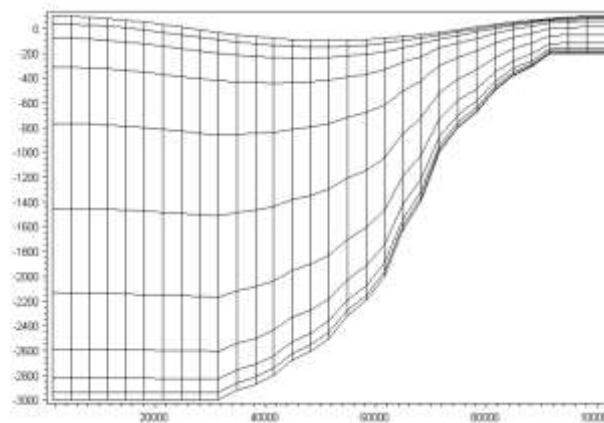


Figure 3.4 Example of vertical distribution using variable distribution. Number of layers: 10, $\sigma_c = 0.1$, $\theta = 5$, $b = 1$

Combined sigma/z-level

In the z-level domain the discretization is given by a number of discrete z-levels $\{z_i, i = 1, (N_z + 1)\}$, where N_z is the number of layers in the z-level domain. z_1 is the minimum z-level, and z_{N_z+1} is the maximum z-level, which is equal to the sigma depth, z_σ . The corresponding layer thickness is given by

$$\Delta z_i = z_{i+1} - z_i \quad i = 1, N_z \tag{3.4}$$

The discretization is illustrated in Figure 3.5 and Figure 3.6.

Using standard z-level discretization the bottom depth is rounded to the nearest z-level. Hence, for a cell in the horizontal mesh with the cell-averaged depth, z_b , each cell in the corresponding column in the z-domain is only included if the following criterion is satisfied

$$z_{i+1} - z_b \geq \frac{1}{2}(z_{i+1} - z_i) \quad i = 1, N_z \quad (3.5)$$

The cell-averaged depth, z_b , is calculated as the mean value of the depth at the vertices of each cell in the horizontal mesh. To take into account the correct depth for the case where the bottom depth is below the minimum z-level ($z_1 > z_b$) a bottom fitted approach is used. Here, a correction factor, f_1 , for the layer thickness in the bottom cell is introduced. The correction factor is used in the calculation of the volume and vertical face integrals. The correction factor for the bottom cell is calculated by

$$f_1 = \frac{(z_2 - z_b)}{\Delta z_1} \quad (3.6)$$

The corrected layer thickness is given by $\Delta z_1^* = f_1 \Delta z_1$. The simple bathymetry adjustment approach is illustrated in Figure 3.5.

For a more accurate representation of the bottom depth an advanced bathymetry adjustment approach can be used. For a cell in the horizontal mesh with the cell-averaged depth, z_b , each cell in the corresponding column in the z-domain is included if the following criterion is satisfied

$$z_{i+1} > z_b \quad i = 1, N_z \quad (3.7)$$

A correction factor, f_i , is introduced for the layer thickness for these cells

$$f_i = \min \left(\max \left(\frac{(z_{i+1} - z_b)}{\Delta z_i}, \frac{z_{min}}{\Delta z_i} \right), 1 \right) \quad i = 2, N_z$$

$$f_i = \max \left(\frac{(z_{i+1} - z_b)}{\Delta z_i}, \frac{z_{min}}{\Delta z_i} \right) \quad i = 1 \quad (3.8)$$

A minimum layer thickness, Δz_{min} , is introduced to avoid very small values of the correction factor. The correction factor is used in the calculation of the volume and vertical face integrals. The corrected layer thicknesses are given by $\{\Delta z_i^* = f_i \Delta z_i, i = 1, N_z\}$. The advanced bathymetry adjustment approach is illustrated in Figure 3.6.

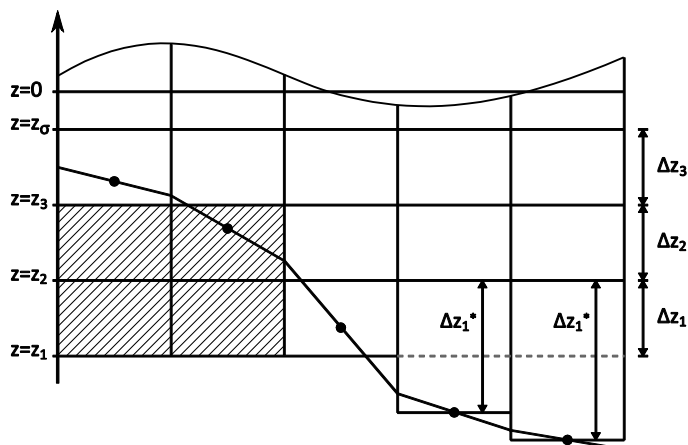


Figure 3.5 Simple bathymetry adjustment approach

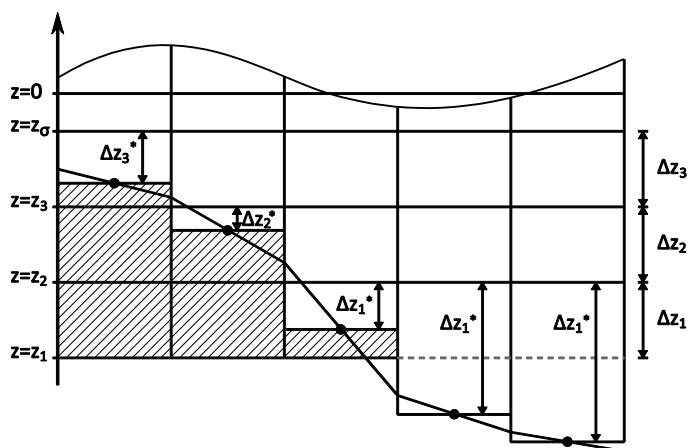


Figure 3.6 Advanced bathymetry adjustment approach

3.1.2 Discretization scheme

The discrete solution for the water depth, h , is defined at the centroid of the elements of the 2D horizontal mesh. The discrete solutions for the velocity components, u , v and w , and the turbulent variables, k and ε , are defined at the centroid of the elements of the 3D mesh. The non-hydrostatic pressure, q , is positioned in the centroid of the horizontal cell faces as shown in Figure 3.7. The location of the discrete non-hydrostatic pressure secures an exact representation of the surface boundary condition. The modified vertical velocity, ω , is also positioned in the centroid of the horizontal cell faces. The coordinates of the centroids are the averages of the coordinates of the cells vertices.

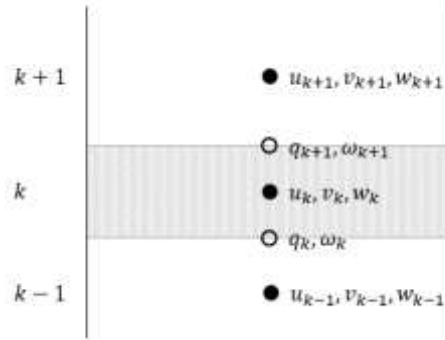


Figure 3.7 Vertical variable arrangement around layer k . Velocity components, u, v and w , are located in cell centers; non-hydrostatic pressure, q , is located in cell interfaces

3.2 Finite volume method

The matrix form of the governing equations presented in Chapter 2 can be written as

$$\frac{\partial \mathbf{U}}{\partial t} + \nabla \cdot \mathbf{F}(\mathbf{U}) = \mathbf{S} \quad (3.9)$$

Integrating Eq. (3.9) over the i th cell and using Gauss's theorem to rewrite the flux integral gives

$$\int_{V_i} \frac{\partial \mathbf{U}}{\partial t} d\Omega + \int_{\Gamma_i} (\mathbf{F}(\mathbf{U}) \cdot \mathbf{n}) d\Gamma = \int_{V_i} \mathbf{S}(\mathbf{U}) d\Omega \quad (3.10)$$

where V_i is the volume of the i th cell, Ω is the integration variable defined on V_i , Γ_i is the boundary of the i th cell and Γ is the integration variable along the boundary. $\mathbf{n} = (n_x, n_y, n_z)^T$ is the unit outward normal vector along the boundary. Evaluating the volume integrals by a one-point quadrature rule, the quadrature point being the centroid of the cell, and evaluating the boundary integral using a mid-point quadrature rule, Eq. (3.10) can be written

$$\frac{\partial \mathbf{U}_i}{\partial t} + \frac{1}{V_i} \sum_j^{NF} \mathbf{F} \cdot \mathbf{n}_{ij} \Delta \Gamma_{ij} = \mathbf{S}_i \quad (3.11)$$

Here \mathbf{U}_i and \mathbf{S}_i , respectively, are average values of \mathbf{U} and \mathbf{S} over the i th cell and stored at the cell centre. NF is the number of faces of the cell and the face ij is common to the cells associated with \mathbf{U}_i and \mathbf{U}_j . $\Delta \Gamma_{ij}$ is the area of the face ij , and \mathbf{n}_{ij} is the restriction of \mathbf{n} to the face ij .

3.3 Numerical solution of the Navier-Stokes equations

3.3.1 Space discretization

The space discretization is performed using the finite volume method as described in Section 3.2. In this section, the focus is on the discretization for the equations in the sigma coordinate system.

The normal convective flux $F_n(\mathbf{U}_L, \mathbf{U}_R) = \mathbf{F}(\mathbf{U}_L, \mathbf{U}_R) \cdot \mathbf{n}_{ij}$ across a vertical face ij is determined using an approximate Riemann solver. The Riemann solver uses the variable $\mathbf{U} = (h, hu, hv, hw)^T$ to the left and right of the face. The convective flux at the horizontal faces is calculated using a second-order upwinding scheme. The diffusive flux at the cell interfaces is approximated by a central scheme. This vertical discretization results in a linear five-diagonal system which has to be solved for each column of the discrete momentum equation.

Reconstruction of face values

The variables, \mathbf{U}_L and \mathbf{U}_R , to the left and right of a face are reconstructed from the cell values, \mathbf{U}_i and \mathbf{U}_j , in two steps.

In the first step, the variables \mathbf{U}_l and \mathbf{U}_r are determined from element values. For a first order scheme, $\mathbf{U}_l = \mathbf{U}_i$ and $\mathbf{U}_r = \mathbf{U}_j$. Second-order spatial accuracy is achieved by employing a linear gradient-reconstruction technique for the primitive variables η , u , v and w . The face value at the vertical faces for a variable q in cell i is obtained by

$$q_l = q_i + \nabla q_i \cdot \mathbf{r}_{if}, \quad q_r = q_j + \nabla q_j \cdot \mathbf{r}_{jf} \quad (3.12)$$

where \mathbf{r}_{if} is the distance vector from the cell centre to the face and ∇q_i is the gradient vector. For estimation of the gradient vector, the Green-Gauss gradient approach is utilized. Here, the procedure proposed by Jawahar and Kamath (2000) is used. This procedure is based on a wide computational stencil to improve accuracy also for meshes with poor connectivity. The vertex (node) value is computed using the pseudo-Laplacian procedure proposed by Holmes and Connell (1989).

For a second-order scheme, the water depth d is also reconstructed at each side of the face using eq. (3.12) and then the total water depths at the left and right of the face are defined as

$$h_l = \max(0, \eta_l + d_l), \quad h_r = \max(0, \eta_r + d_r) \quad (3.13)$$

In the second step, the variables \mathbf{U}_L and \mathbf{U}_R are determined from \mathbf{U}_l and \mathbf{U}_r . The water depth is assigned the same value at both sides of the face, $d_f = d_l = d_r$. Depending on the total water depth, two different techniques are used. As default, the average value of water depth is used

$$d_f = \frac{1}{2}(d_l + d_r) \quad (3.14)$$

and the total water depths are defined by

$$h_L = \max(\eta_l + d_f, 0), \quad h_R = \max(\eta_r + d_f, 0). \quad (3.15)$$

If the total water height on either side is smaller than the difference in water depth, that is, if $h_l < |d_r - d_l|$ or $h_r < |d_r - d_l|$, the water depth is instead defined as in Chen & Noelle (2017) by

$$d_f = -\min(-\min(d_l, d_r), \min(\eta_l, \eta_r)) \quad (3.16)$$

and the total water depths are defined by

$$h_L = \min(\eta_l + d_f, h_l), \quad h_R = \min(\eta_r + d_f, h_r). \quad (3.17)$$

Finally, the fluxes at each side of the face are determined from the velocities $u_l, v_l, w_l, u_r, v_r, w_r$ and the total water depths h_L, h_R .

Riemann solver

The normal convective flux $\mathbf{F}_n(\mathbf{U}) = (f_1, f_2, f_3, f_4)$ at the vertical faces in the sigma domain can be written

$$\mathbf{F}_n(\mathbf{U}) = \begin{pmatrix} hu_{\perp} \\ huu_{\perp} + \frac{1}{2}g(\eta^2 + 2\eta d)n_x \\ hvu_{\perp} + \frac{1}{2}g(\eta^2 + 2\eta d)n_y \\ hwu_{\perp} \end{pmatrix} \quad (3.18)$$

where $\mathbf{U} = (h, hu, hv, hw)^T$ is the solution vector, and $u_{\perp} = un_x + vn_y$ is the velocity perpendicular to the cell face. Here f_1 is the contribution to the continuity equation, and f_2, f_3 and f_4 are the contributions to the three momentum equations. This flux is reconstructed at cell-interfaces using the HLLC scheme introduced by Toro et al. (1994) for solving the Euler equations. The shock-capturing scheme enables robust and stable simulation of flows involving shocks or discontinuities such as bores and hydraulic jumps. This is essential for modelling of waves in the breaking zone or porous structures. The interface flux is computed as follows (see Toro (2001))

$$\mathbf{F}(\mathbf{U}_L, \mathbf{U}_R) \cdot \mathbf{n} = \begin{cases} \mathbf{F}_L & \text{if } S_L \geq 0 \\ \mathbf{F}_{*L} & \text{if } S_L < 0 \leq S_* \\ \mathbf{F}_{*R} & \text{if } S_* < 0 \leq S_R \\ \mathbf{F}_R & \text{if } S_R \leq 0 \end{cases} \quad (3.19)$$

where $\mathbf{F}_L = \mathbf{F}_n(\mathbf{U}_L)$ and $\mathbf{F}_R = \mathbf{F}_n(\mathbf{U}_R)$ are calculated from Eq. (3.18), and the middle region fluxes, \mathbf{F}_{*L} and \mathbf{F}_{*R} are given by

$$\mathbf{F}_{*L} = \begin{pmatrix} e_1 \\ e_2 n_x - u_{\parallel L} e_1 n_y \\ e_2 n_y + u_{\parallel L} e_1 n_x \\ e_3 \end{pmatrix} \quad (3.20)$$

$$\mathbf{F}_{*R} = \begin{pmatrix} e_1 \\ e_2 n_x - u_{\parallel R} e_1 n_y \\ e_2 n_y + u_{\parallel R} e_1 n_x \\ e_3 \end{pmatrix} \quad (3.21)$$

Here $u_{\parallel} = -un_y + vn_x$ is the velocity tangential to the cell face, and (e_1, e_2, e_3) is the component of the normal flux which is calculated using the HLL solver proposed by Harten et al. (1983)

$$\mathbf{E} = \frac{S_R \hat{\mathbf{E}}_L - S_L \hat{\mathbf{E}}_R + f_{HLLC} S_L S_R (\hat{\mathbf{U}}_R - \hat{\mathbf{U}}_L)}{S_R - S_L} \quad (3.22)$$

Here $\hat{\mathbf{U}} = (h, hu_{\perp}, h\omega)^T$ and $\hat{\mathbf{E}} = (hu_{\perp}, hu_{\perp}u_{\perp} + \frac{1}{2}g(\eta^2 + 2\eta d), h\omega)^T$. To be able to scale the damping introduced by the HLLC solver a scaling factor f_{HLLC} has been introduced, where the factor must be in the interval $[0, 1]$. The scaling factor, $f_{HLLC} = 1$, corresponds to the standard HLLC solver.

An appropriate method for approximating the wave speeds is essential for the efficiency of the HLLC solver. Different approximations can be found in the literature, e.g. Fraccarollo and Toro (1994). Here the approach used by Song et al. (2011) is used

$$S_L = \begin{cases} u_{\perp R} - 2\sqrt{gh_R} & h_L = 0 \\ \min(u_{\perp L} - \sqrt{gh_L}, u_{\perp*} - \sqrt{gh_*}) & h_L > 0 \end{cases} \quad (3.23)$$

and

$$S_R = \begin{cases} u_{\perp L} + 2\sqrt{gh_L} & h_R = 0 \\ \max(u_{\perp R} + \sqrt{gh_R}, u_{\perp*} + \sqrt{gh_*}) & h_R > 0 \end{cases} \quad (3.24)$$

where the Roe-averaged quantities

$$u_{\perp*} = \frac{u_{\perp L}\sqrt{h_L} + u_{\perp R}\sqrt{h_R}}{\sqrt{h_L} + \sqrt{h_R}} \quad (3.25)$$

$$h_* = \frac{1}{2}(h_L + h_R) \quad (3.26)$$

The wave speed S_* is given by the

$$S_* = \frac{S_L h_R (u_{\perp R} - S_R) - S_R h_L (u_{\perp L} - S_L)}{h_R (u_{\perp R} - S_R) - h_L (u_{\perp L} - S_L)} \quad (3.27)$$

3.3.2 Time integration

The time integration of the Navier-Stokes equations is performed using a semi-implicit scheme. The vertical convective and diffusive terms are discretized using an implicit scheme to remove the stability limitations associated with the vertical resolution. Here a second order implicit trapezoidal method is used (see Lambert (1973) and Hirsch (1990)). The remaining terms are discretized using a two-stage explicit second-order Runge-Kutta scheme (the midpoint method). The non-hydrostatic pressure is treated by a fractional step approach developed by Chorin (1968) called the projection method which is based on the Helmholtz-Hodge decomposition. In the sigma coordinate system, the integration procedure is

Stage 1:

$$\frac{h^{n+1/2} - h^n}{\Delta t/2} = - \left(\frac{\partial F_x^c}{\partial x'} + \frac{\partial F_y^c}{\partial y'} \right)^n \quad (3.28)$$

$$\frac{\mathbf{U}^* - \mathbf{U}^n}{\Delta t/2} = - \left(\frac{\partial \mathbf{F}_x^m}{\partial x'} + \frac{\partial \mathbf{F}_y^m}{\partial y'} \right)^n - \frac{1}{2} \left(\left(\frac{\partial \mathbf{F}_\sigma^m}{\partial \sigma} \right)^* + \left(\frac{\partial \mathbf{F}_\sigma^m}{\partial \sigma} \right)^n \right) + \mathbf{S}_h^n + \mathbf{S}_q^n \quad (3.29)$$

$$\frac{\mathbf{U}^{n+1/2} - \mathbf{U}^*}{\Delta t/2} = \mathbf{S}_q^* \quad (3.30)$$

Stage 2:

$$\frac{h^{n+1} - h^n}{\Delta t} = - \left(\frac{\partial F_x^c}{\partial x'} + \frac{\partial F_y^c}{\partial y'} \right)^{n+1/2} \quad (3.31)$$

$$\frac{\mathbf{U}^* - \mathbf{U}^n}{\Delta t} = - \left(\frac{\partial \mathbf{F}_x^m}{\partial x'} + \frac{\partial \mathbf{F}_y^m}{\partial y'} \right)^{n+1/2} - \frac{1}{2} \left(\left(\frac{\partial \mathbf{F}_\sigma^m}{\partial z} \right)^* + \left(\frac{\partial \mathbf{F}_\sigma^m}{\partial z} \right)^n \right) + \mathbf{S}_h^{n+1/2} + \mathbf{S}_q^{n+1/2} \quad (3.32)$$

$$\frac{\mathbf{U}^{n+1} - \mathbf{U}^*}{\Delta t} = \mathbf{S}_q^* \quad (3.33)$$

Calculating \mathbf{S}_q^* requires knowledge of the non-hydrostatic pressure, q . The pressure is calculated solving a Poisson equation. The modified vertical velocity is calculated after the update of the water depth from Eq. (2.74).

Due to the explicit scheme, the time step interval, Δt , is restricted by the Courant-Friedrichs-Lewy (CFL) condition

$$C = \Delta t \frac{(\sqrt{gh} + |u|) + (\sqrt{gh} + |v|)}{\Delta l} \leq C_{max} \quad (3.34)$$

where C is the Courant number and Δl is a characteristic length. C_{max} is the maximum Courant number and must be less than or equal to 1. A variable time step interval is used in the time integration of the Navier-Stokes equations and determined so that the Courant number is less than a maximum Courant number in all computational nodes. The characteristic length for a prism, where the horizontal face is a quadrilateral element, is determined as the area of the element divided by the longest edge length of the element. If the horizontal face is a triangular element, the characteristic length is two times the area divided by the longest edge length.

3.3.3 Poisson equation

The Poisson equation is derived by differentiating the three components of the vector Eq. (3.30) and (3.33) by x' , y' and σ and substituting the resulting expressions back into the continuity equation

$$\frac{\partial u}{\partial x'} + \frac{\partial u}{\partial \sigma} \frac{\partial \sigma}{\partial x} + \frac{\partial v}{\partial y'} + \frac{\partial v}{\partial \sigma} \frac{\partial \sigma}{\partial y} + \frac{1}{h} \frac{\partial w}{\partial \sigma} = 0 \quad (3.35)$$

The resulting Poisson equation in sigma coordinates reads

$$\begin{aligned} \frac{\partial^2 q}{\partial x'^2} + \frac{\partial^2 q}{\partial y'^2} + (A_x^2 + A_y^2 + A_z^2) \frac{\partial^2 q}{\partial \sigma^2} + 2A_x \frac{\partial^2 q}{\partial x' \partial \sigma} + 2A_y \frac{\partial^2 q}{\partial y' \partial \sigma} + \\ \left(\frac{\partial A_x}{\partial x'} + \frac{\partial A_y}{\partial y'} \right) \frac{\partial q}{\partial \sigma} = \frac{\rho_0}{\Delta t^*} \left(\frac{\partial u^*}{\partial x'} + \frac{\partial v^*}{\partial y'} + A_x \frac{\partial u^*}{\partial \sigma} + A_y \frac{\partial v^*}{\partial \sigma} + A_z \frac{\partial w^*}{\partial \sigma} \right) \end{aligned} \quad (3.36)$$

In the first stage $\Delta t^* = \Delta t/2$, and in the second stage $\Delta t^* = \Delta t$. The Poisson equation in Cartesian coordinate reads

$$\frac{\partial^2 q}{\partial x^2} + \frac{\partial^2 q}{\partial y^2} + \frac{\partial^2 q}{\partial z^2} = \frac{\rho_0}{\Delta t^*} \left(\frac{\partial u^*}{\partial x} + \frac{\partial v^*}{\partial y} + \frac{\partial w^*}{\partial z} \right) \quad (3.37)$$

The surface and bottom boundary conditions for the non-hydrostatic pressure, q , in the sigma coordinate system are

at $z = \eta$

$$q = 0 \quad (3.38)$$

at $z = -d$

$$\frac{\partial q}{\partial \sigma} = 0 \quad (3.39)$$

For applications where the still water depth, d , is changing in time the following bottom boundary condition is used

$$\frac{\partial q}{\partial \sigma} = \rho_0 h \frac{\partial^2 d}{\partial t^2} \quad (3.40)$$

In a Cartesian coordinate system, the boundary condition at the bottom is

$$\frac{\partial q}{\partial z} = 0 \quad (3.41)$$

Discretization of the Poisson pressure equation is performed by integrating over the individual control volumes. The procedure results in a large sparse linear system that needs to be solved in each of the two stages in the time integration procedure. This sparse linear system of equations is solved using an iterative solver from the PETSc library, Balay (2017). More specifically, the iterative solver is the restarted Generalized Minimal Residual method (GMRES), which for single-subdomain simulations is preconditioned with a two-level incomplete LU factorization, ILU(2). For multi-subdomain simulations the Block Jacobi preconditioner is used, where each block is solved with ILU(2). Each block coincides with the division of variables over the processors. See Chapter 5 for further details on single- and multi-subdomain simulations.

3.3.4 Flooding and drying

The approach for treatment of the moving boundaries (flooding and drying fronts) problem is based on the work by Zhao et al. (1994) and Sleigh et al. (1998). When the depths are small the problem is reformulated, and only when the depths are very small the elements/cells are removed from the calculation. The reformulation is made by setting the momentum fluxes to zero and only taking the mass fluxes into consideration.

The depth in each element is monitored and the elements are classified as dry, partially dry or wet. Also, the element faces are monitored to identify flooded element faces.

- An element face is defined as flooded if the water depth at one side of a face is less than a tolerance depth, h_{dry} , and the water depth at the other side of the face is larger than a tolerance depth, h_{wet} .
- An element is dry if the water depth is less than a tolerance depth, h_{dry} , and none of the element faces are flooded faces. The element is removed from the calculation.
- An element is partially dry if the water depth is larger than h_{dry} and less than a tolerance depth, h_{wet} , or when the depth is less than h_{dry} , and one of the element faces is a flooded face. The momentum fluxes are set to zero, and only the mass fluxes are calculated.
- An element is wet if the water depth is bigger than h_{wet} . Both the mass flux and the momentum flux are calculated.

A non-physical flow across the face will be introduced for a flooded face when the surface elevation in the wet element on one side of the face is lower than the bed level in the partially wet element on the other side. To overcome this problem the face will be treated as a closed boundary (Section 3.3.7).

In case the water depth becomes negative, the water depth is set to zero, and the water is subtracted from the adjacent elements to maintain mass balance. When this occur the water depth at the adjacent elements may become negative. Therefore, an iterative correction of the water depth is applied (max. 100 iterations). Normally only one or a few correction steps are needed.

3.3.5 Sponge layer

Sponge (or absorbing) layers can be used as efficient numerical wave absorbers in wave simulations. These could be set up along model boundaries to provide radiation boundary conditions, which absorb wave energy propagating out of the model area.

The implemented method is based on the sponge layer technique introduced by Larsen and Dancy (1983). In the sponge layer the calculated surface elevation, η , and the velocities u , v and w , are corrected at every time step as

$$\eta = \frac{\eta - \eta^{ref}}{c} + \eta^{ref} \quad u = \frac{u}{c} \quad v = \frac{v}{c} \quad w = \frac{w}{c} \quad (3.42)$$

where c is the sponge coefficient, and η^{ref} is the reference level.

To minimize reflections, the values of the sponge layer coefficient, c , should be close to unity along the front edge of the sponge layer and should increase smoothly towards the closed/land boundary. When selecting the sponge layer coefficient, c , the following formula has been found to work well

$$c = a^{r \cdot s / \Delta s}, \quad 0 \leq s \leq w \quad (3.43)$$

where w is the width of the sponge layer, and a and r are assigned constant values. s is the distance from the closed boundary, and Δs is the characteristic size of the elements in the sponge layer area. Depending on ratio $w/\Delta s$ you may use the values listed in Table 3.1.

Table 3.1 Recommended values for sponge layer coefficients

$w/\Delta s$	a	r
10	5	0.5
20	7	0.7
50	10	0.85
100	10	0.92

200	10	0.95
-----	----	------

3.3.6 Internal wave generation

The relaxation zone technique is applied for wave generation and absorption. Here a relaxation function is applied to introduce the analytical solution for the incoming waves smoothly into the calculation domain. The analytical solution is the target solution and contains values from the chosen wave theory for the surface elevation, the velocities and the pressure. The relaxation zone is defined as the area to the right of the polyline when positioned at the starting point and looking forward along the line (see Figure 3.8). The target and the computed solution are weighted in the relaxation zone after each step in the time integration

$$\theta = \alpha\theta_{Computed} + (1 - \alpha)\theta_{Target} \tag{3.44}$$

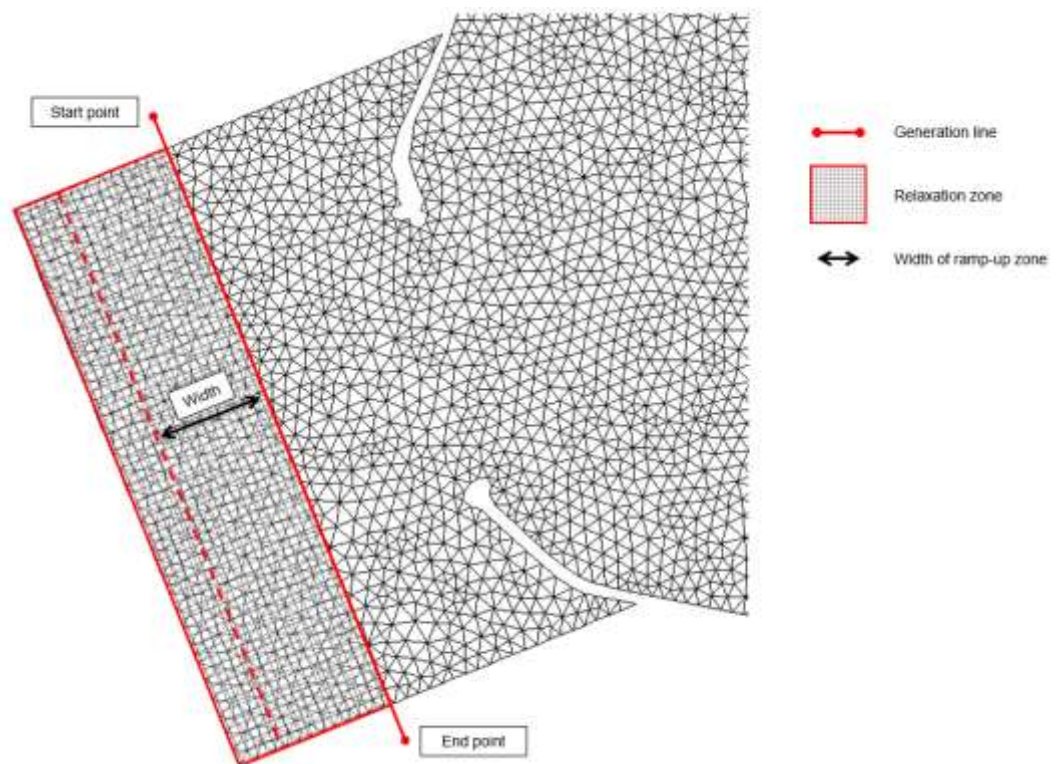


Figure 3.8 The relaxation zone is the area to the right of the generation line when looking forward along the line from the starting point. The width of the ramp-up zone is specified by the width parameter.

where θ represents the surface elevation, velocity component and non-hydrostatic pressure. For the surface elevation and velocities the ramp up factor, α , is given as

$$\alpha = 1 - \frac{\exp(s^f) - 1}{\exp(1) - 1} \quad 0 \leq s \leq 1 \tag{3.45}$$

$$\alpha = 0 \quad s > 1$$

Here, s is the distance from the polyline divided by the width of the ramp up zone, and f is the ramp up factor. The value $f = 3.5$ is applied. For the non-hydrostatic pressure, q , the

target value is applied as a Dirichlet condition for $s > 1$. Hence, here the ramp up factor is given by

$$\begin{aligned} \alpha &= 1 & 0 \leq s \leq 1 \\ \alpha &= 0 & s > 1 \end{aligned} \tag{3.46}$$

For unidirectional regular waves Stokes theory (1th and 5th order) and stream function theory (Fenton (1988)) can be applied. For irregular waves the single summation method is applied. Here a single direction is assigned to each discrete frequency. A range of standard formulations for the frequency spectrum and the directional distribution are applied.

3.3.7 Boundary conditions

At the lateral closed (solid) boundaries, either a condition of zero velocity or a condition of zero normal velocity is imposed. A condition of zero velocity, $u = v = w = 0$, is also called a no-slip condition. For a condition with zero normal velocity, $u_{\perp} = 0$, the normal flux vector is

$$\mathbf{F}_n(\mathbf{U}) = \begin{pmatrix} 0 \\ \frac{1}{2}g(\eta^2 + 2\eta d)n_x \\ \frac{1}{2}g(\eta^2 + 2\eta d)n_y \\ 0 \end{pmatrix} \tag{3.47}$$

For the zero normal velocity condition, a wall friction can be applied, see section 4.3. If the normal velocity is zero and there is no wall friction, the tangential stress is set to zero and this boundary condition is sometimes called a full-slip condition. At the lateral closed boundaries, the normal pressure gradient is zero.

3.4 Numerical solution of the Transport equations

3.4.1 Spatial discretization

Using the first-order scheme for the spatial discretization the normal flux due to the convective terms at the (vertical) faces is calculated using simple upwinding. It is calculated as the mass flux times the concentration at the element in the upwind direction. The numerical damping using the first order scheme is quite high. The advantage is that there is no overshooting or undershooting, which for some applications is very important. Using the second-order scheme for the spatial discretization a higher-order upwind scheme is applied. The concentration at the (vertical) faces is determined using a linear gradient reconstruction technique based on the concentration and the gradient of the concentration at the element in the upwind direction. The gradient is determined using a wide computational stencil (see section 3.3.1). To provide stability and minimize oscillatory effects, the gradient limiter proposed by Barth and Jespersen (1989) is applied to limit the horizontal gradients. This approach significantly reduces the numerical damping compared to the first-order scheme.

When the explicit time integration approach is used for the vertical convective terms, the calculation of the normal flux due to the convective terms at the horizontal faces is performed using a 3rd order ENO procedure (Shu, 1997). When the implicit time

integration approach is used for the vertical convective terms the normal flux is calculated using a first-order upwinding scheme.

3.4.2 Time integration

The time integration is performed using either a first order explicit Euler method or a second-order explicit Runge-Kutta scheme (the midpoint method). However, to overcome the severe time step restriction due to small vertical grid spacing, the vertical convective and diffusive terms are treated implicitly. The vertical diffusion term is treated using a second order implicit trapezoidal method. The vertical convective term is treated either using the explicit method or an implicit Euler method, and the same method is used for all discrete equations in a column of the 3D mesh. The explicit method is used when the following criteria are satisfied

Sigma domain

$$\frac{\omega_i \Delta t}{\Delta \sigma_i} < \frac{1}{2} \quad (3.48)$$

z-level domain

$$\frac{w_i \Delta t}{\Delta z_i} < \frac{1}{2} \quad (3.49)$$

for all elements in the column. Here ω_i is the modified vertical velocity and $\Delta \sigma_i$ the vertical grid spacing in the sigma domain. w_i is the vertical velocity and Δz_i the vertical grid spacing in the z-level domain. Finally, Δt is the discrete time step interval. For details of the time integration methods, see Lambert (1973) and Hirsch (1990).

The transport equations for the turbulence model are solved using the same time step as used for solving the Navier-Stokes equations.

3.4.3 Boundary conditions

Solving the transport equations for the turbulence model, the lateral closed boundary conditions depend on the boundary conditions for the flow equations. In case of no-slip condition or in case of zero normal velocity where wall friction is applied, a Dirichlet boundary condition is applied. The values in the elements at the wall are calculated using the wall functions in eq. (2.59). In this case, $\Delta y = \Delta y_w$ is the distance to the wall from the center of the elements and $U_\tau = U_{\tau w}$ is the friction velocity associated with the wall stress, see section 4.3. In case of zero normal velocity without wall friction, the normal convective flux is zero, and the normal gradient of the transport variables is zero.

3.5 Time stepping procedure

The solution is determined at sequence of discrete times

$$t^k = t^0 + k \Delta t_{overall} \quad k = 0, 1, 2, 3 \dots \quad (3.50)$$

where $\Delta t_{overall}$ is the overall time step interval. The time steps for the hydrodynamic calculations are dynamic.

At the actual time t in the interval $t^{k-1} < t \leq t^k$ the new time step interval is determined using the following procedure

$$\Delta t^* = C_{max} \min \left(\frac{\Delta l}{(\sqrt{gh_i} + |u_i|) + (\sqrt{gh_i} + |v_i|)} \right) \quad (3.51)$$

$$\Delta t^{**} = \min (\max(\Delta t, \Delta t_{min}), \Delta t_{max}) \quad (3.52)$$

$$\Delta t = \frac{t^k - t}{\text{int} \left(\frac{(t^k - t)}{\Delta t^{**}} \right) + 1} \quad (3.53)$$

Here Δt_{min} and Δt_{max} are the minimum and maximum time steps, respectively, and int is the whole number of $(t^k - t)/\Delta t$. This procedure secures that the time steps for the hydrodynamic calculations are synchronized at the overall discrete time steps.

4 Physics

4.1 Eddy viscosity

Both the vertical and horizontal eddy viscosity can be derived solving a turbulence closure model (see section 2.1.2). In that case the eddy viscosity is calculated using eq. (2.18) or (2.39). In some applications, a constant eddy viscosity can be used for the horizontal eddy viscosity. Alternatively, Smagorinsky (1963) proposed to express sub-grid scale transports by an effective eddy viscosity related to a characteristic length scale. The sub-grid scale eddy viscosity is given by

$$\nu_t^h = c_s^2 l^2 \sqrt{2(S_{xx}S_{xx} + 2S_{xy}S_{xy} + S_{yy}S_{yy})} \quad (4.1)$$

where c_s is a constant, l is a characteristic length and the deformation rate is given by

$$S_{xx} = \frac{\partial u}{\partial x} \quad S_{xy} = \frac{1}{2} \left(\frac{\partial u}{\partial y} + \frac{\partial v}{\partial x} \right) \quad S_{yy} = \frac{\partial v}{\partial y} \quad (4.2)$$

For more details on this formulation, the reader is referred to Lilly (1967), Leonard (1974), Aupoix (1984), and Horiuti (1987).

4.2 Bed resistance

The bottom stress, $\boldsymbol{\tau}_b = (\tau_{bx}, \tau_{by})$ is determined by a quadratic friction law

$$\frac{\boldsymbol{\tau}_b}{\rho_0} = c_f \mathbf{u}_b |\mathbf{u}_b| \quad (4.3)$$

where c_f is the drag coefficient, and, \mathbf{u}_b is the flow velocity tangential to the seabed at a distance Δz_b above the bed, and the drag coefficient is determined by assuming a logarithmic profile between the seabed and a point Δz_b above the seabed

$$c_f = \frac{1}{\left(\frac{1}{\kappa} \ln \left(\max \left(\frac{\Delta z_b}{z_0}, 2 \right) \right) \right)^2} \quad (4.4)$$

where $\kappa = 0.41$ is the von Kármán constant, and z_0 is the bed roughness length scale. When the boundary surface is rough, z_0 depends on the roughness height, k_s , trough

$$z_0 = m k_s \quad (4.5)$$

where m is approximately 1/30.

The friction velocity associated with the bottom stress is given by

$$U_{\tau b} = \sqrt{c_f |\mathbf{u}_b|^2} \quad (4.6)$$

A semi-implicit discretization is used to get a stable solution for small water depths, which for element i reads

First stage:

$$\frac{\tau_{bi}^{n+1/2}}{\rho_0} = c_f^n |\mathbf{u}_i^n| \mathbf{u}_i^* \quad (4.7)$$

Second stage:

$$\frac{\tau_{bi}^{n+1}}{\rho_0} = c_f^n |\mathbf{u}_i^{n+1/2}| \mathbf{u}_i^* \quad (4.8)$$

Here the * indicates the provisional value of the velocity.

4.3 Wall friction

For closed lateral boundary with zero normal velocity and wall friction, the stress τ_w tangential to the wall is determined by a quadratic friction law

$$\tau_w = \rho_0 c_f \mathbf{u}_{wall} |\mathbf{u}_{wall}| \quad (4.9)$$

Here, c_f is the drag coefficient and \mathbf{u}_{wall} is the velocity tangential to the wall at a distance Δy_w to the wall; \mathbf{u}_{wall} and Δy_w are evaluated at the cell center. The drag coefficient is given by

$$c_f = \frac{1}{\left(\frac{1}{\kappa} \ln \left(\max \left(\frac{\Delta y_w}{y_0}, 2 \right) \right) \right)^2} \quad (4.10)$$

where $\kappa = 0.41$ is the von Kármán constant and y_0 is the wall roughness length scale given by

$$y_0 = m k_s \quad (4.11)$$

The parameter k_s is a wall roughness height and $m \approx 1/30$. Furthermore, the friction velocity $U_{\tau w}$ at the wall is determined as follows (Fuhrman et. al. (2014)).

$$U_{\tau w} = \sqrt{c_f |\mathbf{u}_{wall}|^2} \quad (4.12)$$

For a closed lateral boundary with zero velocity (i.e., a no-slip condition), the friction velocity can be determined using the law of the wall (Bredberg (2008), Wilcox (1998))

$$\frac{|\mathbf{u}_{wall}|}{U_{\tau w}} = \frac{1}{\kappa} \ln \left(\frac{U_{\tau w} \Delta y_w}{\nu} \right) + B \quad (4.13)$$

Here, ν is the kinematic viscosity of water and $B = 5.1$ is an empirically determined constant. Eq. (4.13) is solved iteratively to find $U_{\tau w}$, the friction velocity at the wall, and this value can be used in the boundary conditions of the turbulence models described in section 2.1.2.

4.4 Vegetation

The vegetation structure is modelled as rigid stems with stem diameter, d_s . The height of the vegetation is h_v .

The effect of the vegetation on the flow characteristics is modelled by inclusion of the following drag force in the momentum equations

$$\mathbf{F}_v = \frac{1}{2} C_D \lambda \mathbf{u} |\mathbf{u}| \quad (4.14)$$

where C_D is the drag coefficient, λ is the frontal area per volume and \mathbf{u} is the flow velocity vector. Here $\lambda = d_s N_v$, where N_v is the vegetation density. The vegetation density is the number of plants per unit area. The force in the vertical direction can be neglected when the vegetation structure is vertical stem or blades.

A layered approach can be used to take into account the vertical variation of the vegetation. The drag coefficient, $C_{D,i}$, the stem diameter, $d_{s,i}$, the vegetation height, $h_{v,i}$, and the vegetation density, $N_{v,i}$, are then specified for each vertical layer, i . The vegetation height is the distance from the bed to the top of the vegetation layer.

For the turbulence model the production term due to vegetation is given by

$$P_v = \frac{1}{2} C_D \lambda |\mathbf{u}|^3 \quad (4.15)$$

Following Lopez and Garcia (1998) the weighting coefficient using the k- ϵ model is set to $c_{fk} = 1$ and $c_{f\epsilon} = c_{2\epsilon}/c_{1\epsilon}$. With the default values for $c_{1\epsilon}$ and $c_{2\epsilon}$ then $c_{f\epsilon} = 1.33$. Using the k- ω model the default values for both c_{fk} and $c_{f\epsilon}$ are set to 1.

4.5 Porosity

For wave simulations, the governing equations have been modified to include porosity and the effects of non-Darcy flow through porous media. In this way, it is possible to model partial reflection, absorption and transmission of wave energy at porous structures such as rubble mound breakwaters.

The main effects of porosity are introduced by additional laminar and turbulent friction terms for describing losses due to flow through a porous structure. In most practical cases the pore sizes are relatively large (typically 0.1m to 1.0m), and the turbulent losses will dominate. The laminar loss term has also been included to allow the simulation of small scale physical model tests.

The flow resistance inside the porous structure is described by the linear and non-linear resistance forces expressed as

$$\mathbf{F} = \rho a \mathbf{u} + \rho b |\mathbf{u}| \mathbf{u} \quad (4.16)$$

where a and b are resistance coefficients accounting for the laminar and turbulent friction loss, respectively, $\mathbf{u} = (u, v, w)$ is the velocity vector, and the magnitude of the flow velocity is defined by $|\mathbf{u}| = \sqrt{u^2 + v^2 + w^2}$. a and b are determined by the empirical expressions formulated by van Gent (1995) and Liu et al. (1999)

$$a = \alpha \frac{(1-n)^2}{n^3} \frac{\vartheta}{D_{50}^2} \quad (4.17)$$

$$b = \beta \left(1 + \frac{7.5}{KC}\right) \frac{(1-n)}{n^2} \frac{1}{D_{50}} \quad (4.18)$$

Where n is the porosity, α and β are user specified coefficients, ϑ is the kinematic viscosity and D_{50} is the grain diameter of the porous materials. KC is the Keulegan-Carpenter number defined as

$$KC = \frac{u_m T}{n D_{50}} \quad (4.19)$$

where u_m is the maximum oscillating velocity, and T is the period of the oscillation. u_m is approximated by the magnitude of the flow velocity.

In the momentum equations the time derivative terms are multiplied by a factor $(1 + C_m)$ where C_m is the added mass coefficient to take transient interaction between grains and water into account. van Gent (1995) gave C_m as

$$c_m = \gamma \frac{1-n}{n} \quad (4.20)$$

where γ is an empirical coefficient, which takes the value 0.34.

In the transport equations for the k - ε model additional production terms are included for porous media flow following the approach by Nakayama and Kuwahara (1999) and Hsu et al. (2002).

In the sigma domain the z-coordinate (in the physical domain) of the element centers is varying in time. Therefore the porosity has to be updated at each calculation step. Here, a bilinear interpolation is applied for mapping the specified porosity map onto the calculation mesh.

5 Parallelization

The MIKE 3 Wave Model FM is parallelized for shared-memory multiprocessor/multicore computers using OpenMP. This parallelization is performed by adding compiler directives to the code. To improve performance and to be able to perform simulations on large massively parallel distributed-memory computers and clusters, MIKE 3 Wave Model FM has also been parallelized using domain decomposition concept and Message Passing Interface (MPI). Given the number of processor cores allocated to a simulation, the computational mesh is partitioned into subdomains, and the workload associated with each domain is distributed between the allocated cores. The data exchange between domains is performed by message passing using the Intel MPI Library, which has multi fabric message passing capabilities. It allows the use of mixed communication between the domains. Thus, domains will exchange data via the fastest communication interface – in ranked order: shared memory, InfiniBand, Ethernet, etc.. The implementation uses a hybrid approach (OpenMP and MPI).

5.1 The domain decomposition

The domain partitioning is performed using the METIS graph partitioning library (Karypis and Kumar, (1998, 1999)). The computational mesh is converted into a graph, and then METIS uses a multi-level graph partitioning scheme to split the graph into subgraphs, representing the partitioned subdomains, which are distributed among the allocated cores. METIS computes a balanced partitioning that minimizes the connectivity of the subdomains. This partitioning is performed based on the 2D (horizontal) mesh. Using a 2D mesh to partition a 3D domain can cause unbalanced partitioning. When combined sigma/z-level discretization is used in 3D flow calculations, the number of vertical elements can vary significantly across the domain. This difference in the number of vertical elements can lead to an unbalanced partitioning. To get a balanced partitioning for a 3D mesh, weights corresponding to the actual number of vertical elements associated to each vertex of the graph are used. The partitioning is then made so that the sum of vertex-weights is the same for all subdomains. Hence, with both 2D and 3D meshes, the partitioning strategy ensures that the difference in the number of elements in all subdomains is minimized.

The chosen numerical scheme for the discretization in the spatial domain requires an overlapping domain decomposition. It is based on the halo-layer (“ghost”-cells) approach, where each subdomain contains elements from connected subdomains. This overlap is needed, because calculations require values from the connecting elements. Thus, calculations of some elements at the border between subdomains require values from the connected subdomains.

5.2 Data exchange

The data exchange between processes is based on the aforementioned halo-layer (“ghost”-cells) approach with overlapping elements. The extension of the halo-layer area depends on the numerical scheme used for the discretization in the spatial domain and which variables are chosen to be exchanged between subdomains. Here a two-element wide halo-layer is applied. The data exchanges are performed via asynchronous communication when possible, and synchronous communications are used in different parts of the system to ensure correct execution. The MIKE 3 Wave Model FM uses a dynamic time step in the time integration scheme. To ensure that the calculations are performed with the same time step in all subdomains, time step information is exchanged between processes and thereby synchronizing the processes of each time step. Several

special features require additional data exchange. These special interest points cause synchronization of two or more subdomains during the data exchange. The case of input and output data exchange is mentioned in the next subsection. Finally, information is exchanged between subdomains in connection with error handling. When the system encounters an error in the model, the error is distributed to the other processes when the time step is finished and the simulation is stopped.

5.3 Input and output

The input and output (I/O) is handled using a parallel I/O approach. The master process reads the global mesh information, performs the partitioning of the mesh and distributes the information about the individual subdomains to the slave processes. Each process then reads the additional input specifications using the generic specification file. The input data (porosity maps, sponge layer maps, etc.) are read by each process using the global data files. Since the individual processes perform I/O locally, the simulation data files must be accessible by each process. This access could be through a network-attached storage system or locally on each computer. The output data files from the simulations are written to private files for each subdomain. At the end of the simulation, the data files are merged to obtain data files containing global information.

6 References

- /1/ Aupoix, B. (1984), Eddy Viscosity Subgrid Scale Models for Homogeneous Turbulence, in Macroscopic Modelling of Turbulent Flow, Lecture Notes in Physics, Proc. Sophie-Antipolis, France.
- /2/ Balay, S. K. (2017), *PETSc User Manual*, Tech. Rep. ANL-95/11-Revision 3.8, Mathematics and Computer Science Division., Argonne National Lab.
- /3/ Bredberg, J. (2000). On the wall boundary condition for turbulence models. *Chalmers University of Technology, Department of Thermo and Fluid Dynamics. Internal Report 00/4. Göteborg*, 8-16.
- /4/ Chen, G., & Noelle, S. (2017). *A new hydrostatic reconstruction scheme based on subcell reconstructions*. *SIAM Journal on Numerical Analysis*, 55(2), 758-784.
- /5/ Chippada, S., Dawson, C.N., Martinez, M.L. and Wheeler, M.F. (1998), *A Godunov-type finite volume method for the system of Shallow Water Equations*, *Computational Methods in Applied Mechanics and Engineering*, 151, 105-129.
- /6/ Chorin, A. J. (1968), *Numerical Solution of the Navier-Stokes Equations*, *Math. Comp.*, 22.
- /7/ Fenton, J. D. (1988), *The numerical solution of steady water wave problems*, *Computers & Geosciences*, Vol. 14, No. 3, pp 357-368.
- /8/ Fraccarollo I., Toro E.F. (1994), *Experimental and numerical assessment of the shallow water model for two-dimensional dam-break type problems*, *Journal of Hydraulic Research* 33, 951-979.
- /9/ Fuhrman, D. R., Baykal, C., Sumer, B. M., Jacobsen, N. G., & Fredsøe, J. (2014). Numerical simulation of wave-induced scour and backfilling processes beneath submarine pipelines. *Coastal engineering*, 94, 10-22.
- /10/ Harten A., Lax P.D., Van Leer B. (1983), *On upstream differencing and Godunov-type schemes for hyperbolic conservation-laws*, *SIAM Rev* 25(1), 54-74.
- /11/ Hirsch, C. (1990). *Numerical Computation of Internal and External Flows*, Volume 2: Computational Methods for Inviscid and Viscous Flows, Wiley.
- /12/ Holmes, D. G. and Connell, S. D. (1989), *Solution of the 2D Navier-Stokes on unstructured adaptive grids*, AIAA Pap. 89-1932 in Proc. AIAA 9th CFD Conference.
- /13/ Horiuti, K. (1987), Comparison of Conservative and Rotational Forms in Large Eddy Simulation of Turbulent Channel Flow, *Journal of Computational Physics*, 71, pp 343-370.
- /14/ Hsu T.-J., Sakakiyama T., Liu P.L.-F. (2002), *A numerical model for wave motions ad turbulent flows in front of a composite breakwater*, *Coastal Eng.* 55, 1148-1158.
- /15/ Jawahar P. and Kamath H. (2000), *A high-resolution procedure for Euler and Navier-Stokes computations on unstructured grids*, *Journal of Computational Physics*, 164, 165-203.

- /16/ Karypis G., Kumar .V. (1998), *METIS: family of multilevel partitioning algorithms*, Available from: <http://glaros.dtc.umn.edu/gkhome/views/metis>
- /17/ Karypis G., V. Kumar (1999), *A Fast and Highly Quality Multilevel Scheme for Partitioning Irregular Graphs*, SIAM Journal on Scientific Computing, Vol. 20, No. 1, 1999, pp. 359—392.
- /18/ Lambert J.D. (1973), *Computational Methods in ordinary Differential Equations*, John Willey & Sons.
- /19/ Larsen, B. E., & Fuhrman, D. R. (2018). On the over-production of turbulence beneath surface waves in Reynolds-averaged Navier–Stokes models. *Journal of Fluid Mechanics*, 853, 419-460.
- /20/ Larsen, J., & Dancy, H. (1983), *Open Boundaries in Short-wave Simulations - A New Approach*, Coastal Engineering, 7, 285-297.
- /21/ Leonard, A. (1974), Energy Cascades in Large-Eddy Simulations of Turbulent Fluid Flows, *Advances in Geophysics*, 18, pp 237-247.
- /22/ Liang Q., Borthwick A.G.L, (2009), *Adaptive quadtree simulation of shallow flows with wet-dry fronts over complex topography*, Computers and Fluids 38, 221-234.
- /23/ Lilly, D.K. (1966), On the Application of the Eddy Viscosity Concept in the Inertial Subrange of Turbulence, NCAR Manuscript No. 123, National Center for Atmospheric Research, Boulder, Colorado.
- /24/ Lopez, F., Garcia, M. (1998), Open-channel flow through simulated vegetation: suspended sediment transport modeling, *Water Resources Research* 34 (9), 2341–2352.
- /25/ Nakayama A., Kuwahara F. (1999), *A Macroscopic Turbulence Model for Flow in a Porous Medium*, *Journal of Fluid Eng.*, 121, 427-422
- /26/ Quecedo, M. and Pastor, M. (2002), *A reappraisal of Taylor-Galerkin algorithm for drying-wetting areas in shallow water computations*, *International Journal for Numerical Methods in Fluids*, 38, 515-531.
- /27/ Rodi, W. (1984), *Turbulence models and their applications in hydraulics*, IAHR, Delft, the Netherlands.
- /28/ Rodi, W. (1980), *Turbulence Models and Their Application in Hydraulics – A State of the Art Review*, Special IAHR Publication.
- /29/ Rogers, B., Fujihara, M. and Borthwick, A.G.L. (2001), *Adaptive Q-tree Godunov-type scheme for shallow water equations*, *International Journal for Numerical Methods in Fluids*, 35, 247-280.
- /30/ Shu C.W. (1997), *Essentially Non-Oscillatory and Weighted Essentially Non-Oscillatory Schemes for Hyperbolic Conservation Laws*, NASA/CR-97-206253, ICASE Report No. 97-65, NASA Langley Research Center, pp. 83.
- /31/ Sleight, P.A., Gaskell, P.H., Bersins, M. and Wright, N.G. (1998), *An unstructured finite-volume algorithm for predicting flow in rivers and estuaries*, *Computers & Fluids*, Vol. 27, No. 4, 479-508.

- /32/ Smagorinsky J. (1963), *General Circulation Experiment with the Primitive Equations*, Monthly Weather Review, 91, No. 3, 99-164.
- /33/ Song, L. Zhou J., Guo J., Zou Q., and Liu Y. (2011), *A robust well-balanced finite volume model for shallow water flows with wetting and drying over irregular terrain*, Advances in Water Resources, vol. 34, no. 7, 915–932.
- /34/ Song, Y and Haidvogel D. (1994), *A semi-implicit ocean circulation model using a generalized topography-following coordinate system*, Journal of Comp. Physics, 115, pp. 228-244.
- /35/ Toro, E.F. (2001), *Shock-capturing methods for free-surface flows*, Chichester, John Wiley & Sons.
- /36/ Toro, E.F., Spruce, M., Speares, W. (1994). Restoration of the contact surface in the HLL-Riemann solver. Shock Waves 4, 25–34.
- /37/ van Gent, M. R. A. (1995), *Wave Interaction with Permeable Coastal Structures*, (Ph.D. thesis), Delft University.
- /38/ Wilcox, D. C. (1998). *Turbulence modeling for CFD* (Vol. 2, pp. 103-217). La Canada, CA: DCW industries.
- /39/ Wilcox, D. C. (2008). Formulation of the kw turbulence model revisited. *AIAA journal*, 46(11), 2823-2838.
- /40/ Zhao, D.H., Shen, H.W., Tabios, G.Q., Tan, W.Y. and Lai, J.S. (1994), *Finite volume 2-dimensional unsteady-flow model for river basins*, Journal of Hydraulic Engineering, ASCE, 1994, 120, No. 7, 863-833.

APPENDICES

APPENDIX A – Governing equations in spherical coordinates

A Governing equations in spherical coordinates

In spherical coordinates the independent variables in the horizontal domain are the longitude, λ , and the latitude, ϕ . The horizontal velocity field (u,v) is defined by

$$u = R \cos \phi \frac{d\lambda}{dt} \quad v = R \frac{d\phi}{dt} \quad (\text{A1.1})$$

where R is the radius of the earth.

A.1 Governing equations in spherical coordinate system and z-coordinates

A.1.1 Navier-Stokes equations

The continuity and momentum equations are given as

$$\frac{1}{R \cos \phi} \left(\frac{\partial u}{\partial \lambda} + \frac{\partial v \cos \phi}{\partial \phi} \right) + \frac{\partial w}{\partial z} = 0 \quad (\text{A1.2})$$

$$\frac{\partial u}{\partial t} + \frac{1}{R \cos \phi} \left(\frac{\partial u^2}{\partial \lambda} + \frac{\partial v u \cos \phi}{\partial \phi} \right) + \frac{\partial w u}{\partial z} = \quad (\text{A1.3})$$

$$\left(f + \frac{u}{R} \tan \phi \right) v - \frac{1}{R \cos \phi} \left(\frac{1}{\rho_0} \frac{\partial q}{\partial \lambda} + g \frac{\partial \eta}{\partial \lambda} \right) + F_u + \frac{\partial}{\partial z} \left(\nu_t^v \frac{\partial u}{\partial z} \right)$$

$$\frac{\partial v}{\partial t} + \frac{1}{R \cos \phi} \left(\frac{\partial u v}{\partial \lambda} + \frac{\partial v^2 \cos \phi}{\partial \phi} \right) + \frac{\partial w v}{\partial z} = \quad (\text{A1.4})$$

$$- \left(f + \frac{u}{R} \tan \phi \right) u - \frac{1}{R \cos \phi} \left(\frac{1}{\rho_0} \frac{\partial q}{\partial \phi} + g \frac{\partial \eta}{\partial \phi} \right) + F_v + \frac{\partial}{\partial z} \left(\nu_t^v \frac{\partial v}{\partial z} \right)$$

$$\frac{\partial w}{\partial t} + \frac{1}{R \cos \phi} \left(\frac{\partial u w}{\partial \lambda} + \frac{\partial v w \cos \phi}{\partial \phi} \right) + \frac{\partial w^2}{\partial z} = - \frac{1}{\rho_0} \frac{\partial q}{\partial z} + F_w + \frac{\partial}{\partial z} \left(\nu_t^v \frac{\partial w}{\partial z} \right) \quad (\text{A1.5})$$

A.1.2 Transport equations

The transport equations for the k - ε model are given as

$$\frac{\partial k}{\partial t} + \frac{1}{R \cos \phi} \left(\frac{\partial u k}{\partial \lambda} + \frac{\partial v k \cos \phi}{\partial \phi} \right) + \frac{\partial w k}{\partial z} = F_k + \frac{\partial}{\partial z} \left(\frac{\nu_{t0}^v}{\sigma_k^v} \frac{\partial k}{\partial z} \right) + P_k - \varepsilon \quad (\text{A1.6})$$

$$\frac{\partial \varepsilon}{\partial t} + \frac{1}{R \cos \phi} \left(\frac{\partial u \varepsilon}{\partial \lambda} + \frac{\partial v \varepsilon \cos \phi}{\partial \phi} \right) + \frac{\partial w \varepsilon}{\partial z} = F_\varepsilon + \frac{\partial}{\partial z} \left(\frac{\nu_{t0}^v}{\sigma_\varepsilon^v} \frac{\partial \varepsilon}{\partial z} \right) + P_\varepsilon - c_{2\varepsilon} \frac{\varepsilon^2}{k} \quad (\text{A1.7})$$

The transport equations for the k - ω model are given as

$$\frac{\partial k}{\partial t} + \frac{1}{R \cos \phi} \left(\frac{\partial uk}{\partial \lambda} + \frac{\partial vk \cos \phi}{\partial \phi} \right) + \frac{\partial wk}{\partial z} = F_k + \frac{\partial}{\partial z} \left(\frac{v_{t0}^v}{\sigma_k^v} \frac{\partial k}{\partial z} \right) + P_k - \beta_k \omega k \quad (\text{A1.8})$$

$$\frac{\partial \omega}{\partial t} + \frac{1}{R \cos \phi} \left(\frac{\partial u \omega}{\partial \lambda} + \frac{\partial v \omega \cos \phi}{\partial \phi} \right) + \frac{\partial w \omega}{\partial z} = F_\omega + \frac{\partial}{\partial z} \left(\frac{v_{t0}^v}{\sigma_\omega^v} \frac{\partial \omega}{\partial z} \right) + F_{\omega c} + P_\omega - \beta_\omega \omega^2 \quad (\text{A1.9})$$

A.2 Governing equations in spherical coordinate system and sigma coordinates

A.2.1 Navier-Stokes equations

The continuity and momentum equations are given as

$$\frac{\partial h}{\partial t'} + \frac{1}{R \cos \phi} \left(\frac{\partial hu}{\partial \lambda'} + \frac{\partial hv \cos \phi}{\partial \phi'} \right) + \frac{\partial \omega}{\partial \sigma} = 0 \quad (\text{A1.10})$$

$$\frac{\partial hu}{\partial t'} + \frac{1}{R \cos \phi} \left(\frac{\partial hu^2}{\partial \lambda'} + \frac{\partial hv u \cos \phi}{\partial \phi'} \right) + \frac{\partial h \omega u}{\partial \sigma} = \quad (\text{A1.11})$$

$$\left(f + \frac{u}{R} \tan \phi \right) hv - \frac{1}{R \cos \phi} \left(\frac{h}{\rho_0} \left(\frac{\partial q}{\partial \lambda} + \frac{\partial q}{\partial \sigma} \frac{\partial \sigma}{\partial \lambda} \right) + gh \frac{\partial \eta}{\partial \lambda} \right) + h F_u + \frac{\partial}{\partial \sigma} \left(\frac{v_t^v}{h} \frac{\partial u}{\partial \sigma} \right)$$

$$\frac{\partial hv}{\partial t'} + \frac{1}{R \cos \phi} \left(\frac{\partial hu v}{\partial \lambda'} + \frac{\partial hv^2 \cos \phi}{\partial \phi'} \right) + \frac{\partial h \omega v}{\partial \sigma} = \quad (\text{A1.12})$$

$$- \left(f + \frac{u}{R} \tan \phi \right) hu - \frac{1}{R} \left(\frac{h}{\rho_0} \left(\frac{\partial q}{\partial \phi} + \frac{\partial q}{\partial \sigma} \frac{\partial \sigma}{\partial \phi} \right) + gh \frac{\partial \eta}{\partial \phi} \right) + h F_v + \frac{\partial}{\partial \sigma} \left(\frac{v_t^v}{h} \frac{\partial v}{\partial \sigma} \right)$$

$$\frac{\partial hw}{\partial t'} + \frac{1}{R \cos \phi} \left(\frac{\partial hu w}{\partial \lambda'} + \frac{\partial hv w \cos \phi}{\partial \phi'} \right) + \frac{\partial h \omega w}{\partial \sigma} = \quad (\text{A1.13})$$

$$- \frac{1}{\rho_0} \frac{\partial q}{\partial \sigma} + h F_w + \frac{\partial}{\partial \sigma} \left(\frac{v_t^v}{h} \frac{\partial w}{\partial \sigma} \right)$$

The vertical velocity, ω , is given by

$$\omega = \frac{1}{h} \left(w + \frac{u}{R \cos \phi} \frac{\partial d}{\partial \lambda} + \frac{v}{R} \frac{\partial d}{\partial \phi} - \sigma \left(\frac{\partial h}{\partial t} + \frac{u}{R \cos \phi} \frac{\partial h}{\partial \lambda} + \frac{v}{R} \frac{\partial h}{\partial \phi} \right) \right) \quad (\text{A1.14})$$

A.2.2 Transport equations

The transport equations for the k - ε model are given as

$$\frac{\partial hk}{\partial t'} + \frac{1}{R \cos \phi} \left(\frac{\partial huk}{\partial \lambda'} + \frac{\partial hv k \cos \phi}{\partial \phi'} \right) + \frac{\partial h \omega k}{\partial \sigma} \quad (\text{A1.15})$$

$$= h F_k + \frac{\partial}{\partial \sigma} \left(\frac{v_{t0}^v}{h \sigma_k^v} \frac{\partial k}{\partial \sigma} \right) + h (P_k - \varepsilon)$$

$$\begin{aligned}
 & \frac{\partial h\varepsilon}{\partial t'} + \frac{1}{R\cos\phi} \left(\frac{\partial hu\varepsilon}{\partial \lambda'} + \frac{\partial hv\varepsilon\cos\phi}{\partial \phi'} \right) + \frac{\partial hw\varepsilon}{\partial \sigma} \\
 & = hF_\varepsilon + \frac{\partial}{\partial \sigma} \left(\frac{v_{t0}^v}{h\sigma_\varepsilon^v} \frac{\partial \varepsilon}{\partial \sigma} \right) + h \left(P_\varepsilon - c_{2\varepsilon} \frac{\varepsilon^2}{k} \right)
 \end{aligned}
 \tag{A1.16}$$

The transport equations for the k - ω model are given as

$$\begin{aligned}
 & \frac{\partial hk}{\partial t'} + \frac{1}{R\cos\phi} \left(\frac{\partial huk}{\partial \lambda'} + \frac{\partial hvk\cos\phi}{\partial \phi'} \right) + \frac{\partial hw_s k}{\partial \sigma} \\
 & = hF_k + \frac{\partial}{\partial \sigma} \left(\frac{v_{t0}^v}{h\sigma_k^v} \frac{\partial k}{\partial \sigma} \right) + h(P_k - \beta_k \omega k)
 \end{aligned}
 \tag{A1.17}$$

$$\begin{aligned}
 & \frac{\partial h\omega}{\partial t'} + \frac{1}{R\cos\phi} \left(\frac{\partial hu\omega}{\partial \lambda'} + \frac{\partial hv\omega\cos\phi}{\partial \phi'} \right) + \frac{\partial hw_s \omega}{\partial \sigma} \\
 & = hF_\omega + \frac{\partial}{\partial \sigma} \left(\frac{v_{t0}^v}{h\sigma_\omega^v} \frac{\partial \omega}{\partial \sigma} \right) + hF_{\omega c} + h(P_\omega - \beta_\omega \omega^2)
 \end{aligned}
 \tag{A1.18}$$

Note that in eqs. (A1.17)-(A1.18), the modified vertical velocity in the sigma coordinate system is called w_s (instead of ω). This is to distinguish it from the specific dissipation rate, ω , of turbulent kinetic energy which was introduced in section 2.1.2.